Republic of Iraq
Ministry of Higher Education and Scientific Research
University of Misan/Collage of Engineering
Department of Electrical Engineering

AN IMPROVED TECHNIQUE FOR SUPPORTING THE PREDICTION OF COMMUNICATION SIGNAL

By

Nabaa Ali Abdullrazaq

B.Sc. electrical engineering, 2011

A THESIS

Submitted in Partial Fulfillment of the

Requirements for the Degree of

Master of Science/ Master in Electrical Engineering

Advisor Name: Assist. prof. Dr. Hasanain Abbas Hasan

2024 A.D 1446 A.H

AN IMPROVED TECHNIQUE FOR SUPPORTING THE PREDICTION OF COMMUNICATION SIGNAL

By

Nabaa Ali Abdullrazaq

Thesis Advisor: Assist. prof. Dr. Hasanain Abbas Hasan

A Thesis Presented
in Partial Fulfillment of the Requirements for the
Degree of Master of Science /Master in Electrical Engineering
August 2024

2024 A.D 1446 A.H

بسم الله الرحمن الرحيم

يَرْفَعِ اللَّهُ الَّذِينَ آمَنُوا مِنكُمْ وَالَّذِينَ أُوتُوا الْعِلْمَ دَرَجَاتٍ ۚ وَاللَّهُ بِمَا تَعْمَلُونَ خَبِيرٌ

[المجادلة : 11]

Abstract

Radio propagation prediction is the process of anticipating how radio signals behave as they travel through the vacuum or atmosphere from one point to another. Accurate propagation models are essential for designing and optimizing wireless networks. However, many theoretical, empirical, and site-specific models have limitations that restrict their usefulness in this regard.

To calculate the signal strength at the receiver, it is necessary to predict path loss using radio propagation prediction models. A recent thesis proposed a propagation model that provides good accuracy for 3G and 4G communications in Iraq/ Misan Governorate /Amarah city. The thesis covered four different location zones within Amarah city. These sites vary with buildings and population density. This region is known for its tropical and wet climate and has various buildings of different heights, ranging from one to three stories.

The data was collected using the Drive Test feature of the Test Mobile Phone (TEMS) phone connected to the TEMS investigation tool. The proposed model provided better results than other empirical propagation models mentioned in this thesis. The model showed root mean square error (RMSE) less than other models (FSPL, Hata and Cost231-Hata) at mobile antenna heights of 1.0m and distances of 40, 200, 400, and 600 meters between transmitter and receiver. The RMSE for distance 600 meter is between $2.3 \leq \text{RMSE} \leq 5.3$. These findings will help optimize system performance by revamping radio frequency planning and system design, minimizing network inherent failings such as missed calls, quality issues, handover, and related issues.

The proposed model can be used for path loss prediction and channel characterization, involving the use of similar channel parameters to analyze wireless communication in different mobile environments. Other propagation

models, such as Hata and COST231, that over-predicted the radio channel may need further investigation in the future. The analysis indicated that the RMSE was within the permissible limits of the study.

The study employed several software packages, including TEMS, MapInfo, Google Earth Pro, and MATLAB program 2020, for field measurements, data processing, simulation, and analysis of the results.

SUPERVISOR CERTIFICATION

I certify that the preparation of this thesis entitled " **An Improved Technique for Supporting the Prediction of Communication Signal** " was presented by " **Nabaa Ali Abdullrazaq** ", and prepared under my supervision at the University of Misan, Department of Electrical Engineering, College of Engineering, as partial fulfillment of the requirements for the degree of Master of Science in Electrical Engineering (Communications Engineering).

Signature:

Assist. prof. Dr. Hasanain Abbas Hasan

Date:

In view of the available recommendations, I forward this thesis for discussion by the examining committee.

Signature:

Head of Electrical Eng. Deparment:

Assist. prof. Dr. Mohammed Kh. AL-Nussairi

Date:

EXAMINING COMMITTTEE’S REPORT

We certify that we, the examining committee, have read the thesis titled **(An Improved Technique for Supporting the Prediction of Communication Signal)** which is being submitted by (**Nabaa Ali Abdullrazaq**), and examined the student in its content and in what is concerned with it, and that in our opinion, it meets the standard of a thesis for the degree of Master of Science in Electrical Engineering (Communications).

Signature:

Name: Associate. Prof. Dr. Hasanain Abbas Hasan

(Supervisor)

Date: / / 2024

Signature:

Name:

( ) ( )

Date: / / 2024

Signature:

Name:

( )

Date: / / 2024

Approval of the College of Engineering:

Signature:

Name:

Dean, College of Engineering

Date: / / 2024

DEDICATION

To those who carried the doubt of science, and spread over the universe, the prophet Mohammad, and his family .

To that person I miss his applause in joy at my achievement at this moment, but I never miss the prayers that I reap every moment,to the soul of my father, who went up to her God.

To whom I have always raised my head proudly, to my mother.

To my husband who participated with me in the study march.

To my brothers, sisters, and friends whose encouraged me to complete my studies

To all of these I am grateful to you

ACKNOWLEDGEMENTS

I am grateful to Allah for his blessings as I pursued my academic studies. I want to thank my supervisor, Associate. prof. Dr. Hasanain A. Hasan, sincerely for his counsel, support, and assistance during the writing of my thesis. I also want to express my gratitude to the staff at the Electrical Engineering Department.

Throughout my academic journey, my family and friends have supported me with love, sacrifice, and patience, and for that, I am very grateful.

Table of Contents

LIST OF TABLES

LIST OF FIGURES

LIST OF SYMBOLS

A, B and C	Terrain type
a, b and c	Model constants
Ae	Effective aperture of receive antenna (meter2)
c	Speed of light (m/sec).
d	Distance (meter or kilometer)
d1	Distance between transmitter and obstruction (meter)
d2	Distance between obstruction and receiver (meter)
dd	Distance traveled by wave (meter)
Dn	Diffraction coefficient for nth diffraction object on the ray path
do	Close path distance (meter)
dr	Distance traveled by wave including reflection path (meter)
E	Electric field intensity (V/m)
Ed	Diffracted E-field component (V/m)
Ei	Incident electric field intensity (V/m)
Eo	Peak value of the E-field (V/m)
Er	Reflected electric field intensity (V/m)
ETOT	Total received electric field intensity (V/m)
EG	Ground reflected electric field intensity (V/m)
ELOS	LOS received electric field intensity (V/m)
f	Frequency of the propagating signal (MHz)
Garea	Gain related to environment type (dB)
Ghb	Gain due to mobile height (dB)
Ghm	Gain due to base station height (dB)
GR	Antenna gain of the receiver antenna

GT	Antenna gain of the transmitter antenna
hb	Base station antenna height (meter)
hec	Increase in object's height due to earth curvature effect (meter)
hm	Mobile antenna height (meter)
Jo	Bessel function of the first kind and zero order
k	Constant related to Eo
L	Path Loss (dB)
L_d	Diffraction loss (dB)
L_f	Free Space Path Loss (dB)
Lrural	Median path loss in rural area (dB)
Lsuburban	Median path loss in suburban area (dB)
Lurban	Median path loss in urban area (dB)
p_i	Value of The Actual Receiver Power
$\tilde{p}_I$	Value of The Predicted Receiver Power
P_R	Received power (Watt)
P_T	Transmitted power (Watt)
$p_{Loss}^{CI}(f, d)$	The PL between the existing TX-Rx spaces at the considered frequency
re	Effective earth radius (kilometer)
Γi	Reflection coefficient for the ith reflection surface on the ray path
s	Lognormal-distributed path loss factor with a standard deviation of 8.2 to 10.6 dB
Sav	Average power density (W/m)
Sl	Scattering coefficient of the lth scattering surface on the ray path
T	Transmission coefficient

T_k	Wall transmission coefficient of the kth wall on the ray path
$X\sigma$	Lognormal-distributed random variable with zero mean and standard deviation of σ
Γ	Reflection coefficient
Δd	Distance difference between dd and dr (meter)
$\Delta\theta$	Phase difference between dd and dr (radians)

LIST OF ABBREVIATIONS

ADI-PE	Alternating Direction-Implicit Parabolic Equation
AI	Artificial intelligent
ANN	Artificial Neural Network
BER	Bit Error Rate
CNN	Convolutional Neural Network
DEM	Digital Elevation Map
DL	Deep Learning
DNN	Deep Neural Network
DT	Drive Test
EM	Electromagnetic Wave
ELM	Extreme Learning Machine
ETRT	Effective three-dimensional ray tracing
FCC	Federal Communications Commission
FDTD	Finite-Difference Time-Domain
GIS	Geographic Information System
GLM	Generalized Linear Model
GO	Geometric Optics
GPS	Global Positioning System
GRNN	Generalized Regression Neural Network
GRU	Gated Recurrent Units
GSM	Global System for Mobile Communications
HF	High Frequency
HO	Horoscope
HP	Horizontal polarization wave

IoT	Internet of Things
IMT-2000	International Mobile Telecommunications
ITU	International Telecommunication Union
KNN	K Nearest Neighbor
LMBP	Levenberg Marquardt Back Propagation
LOS	Line-of-sight
LSTM	Long Short Term Memory
LTE	Long Term Evolution
MAE	Mean Absolute Error
ML	Machine Learning
MLP	Multilayer Perceptron
MMDS	Multipoint, Multichannel Distribution Service
MSE	Mean Sequare Error
NN	Neural Network
NLOS	Non line-of-sight
PCA	Principal Component Analysis
PCD	Point Cloud Data
PCS	Personal Communications Service
QoS	Quality of Service
RE	Relative Error
RF	Radio Frequency
RMSE	Root Mean Sequare Error
RSS	Received Signal Strength
RT	Ray tracing

RTT	Real Time Text
SBR	Shooting Bouncing Ray
SNR	Signal to Noise Ratio
SRTM	Shuttle Radar Topography Mission
SUI	Stanford University Interim
SVR	Support Vector Regression
TEMS	Test Mobile System
UAV	Unmanned Aerial Vehicles
UHF	Ultra-High Frequency
UMTS	Universal Mobile Telecommunications System
UTD	Uniform Theory of Diffraction
UWB	Ultra-Wide-Band
VHF	Very High Frequency
VP	Vertical polarization wave
WCDMA	Wideband Code division Multiple Access

Chapter One : INTRODUCTION

1.1 General Introduction

Modern life heavily rely on mobile wireless communication services [1]. With unrestricted global communication, it facilitates human commerce, lifestyle, and social interaction [2]. Companies and operators offer these wireless network services, which range from non-real time activities like web browsing to real-time ones like phone and video calls [3]. Thanks to these performance measures, wireless network operators will be able to maintain and improve network performance while staying within acceptable bounds performance measures for both real-time and non-real-time services [4]. By attracting more users and consequently more assets, this respectable performance will keep them from breaking the license regulatory contract.

One important performance metric is the network's ability to accurately predict signal propagation in the wireless network, which depends on the network's design. The main advantage of prediction is that it is used for planning and optimization the network [5].

The accuracy of propagation models varies significantly when used in different environments. This discrepancy is due to the fact that the application context of the propagation model differs from the environment in which it was developed. In some countries, using these models leads to disappointing and misleading results, which can result in inadequate network design [6].

When used in specific scenarios, such as in Japanese cities, certain commonly utilized propagation models like Okumura, Hata, and others, can offer exceptionally accurate results. However, when applied in different settings, like European cities, they may result in significant errors[7].

Other models in the site-specific class, such as Finite-Difference Time-Domain (FDTD), can provide extremely precise findings regardless of the propagation environment. However, their applications are limited by the significant computation and lengthy prediction times required for small areas [8].

This thesis produce an empirical model that is accurate enough for use in Amarah city to build and optimize wireless networks.

1.2 Radio Wave Propagation

Wave propagation refers to the behavior of a wave as it travels from the transmitter to the receiver in a specific environment. Similar to light waves, radio waves are influenced by diffraction, reflection, scattering, absorption, and refraction processes. Understanding how each of these phenomena affect in radio waves is essential for tasks such as choosing broadcast frequencies, designing mobile wireless communication systems, utilizing radio navigation, and operating radar equipment [9].

A line-of-sight (LOS) connection between the transmitter and receiver may or may not exist in the majority of mobile wireless communication systems that operate in urban, suburban, rural, and open regions. When there is no clear line of sight and obstructions like mountains, hills, buildings, and trees are present, there is considerable diffraction loss. Due to reflections of the objects in the propagation path, electromagnetic waves move along distinct paths of variable lengths. The interaction between these waves can lead to multipath fading at specific locations, which causes the power of the received waves to decrease as the separation distance between the transmitter and receiver grows [10].

Propagation models can be used to estimate and anticipate the received signal strength as a function of the transmitter's distance. As a result, the use of propagation models that predict the mean signal level can be used to determine the coverage area of a transmitter at a specific location [11]. Given that they estimate the signal strength across a distance of hundreds or thousands of meters, this type of propagation modeling is on a huge scale (large scale propagation model) . Another class of propagation models is the fading model (or small-scale model), which describes the abrupt changes in signal strength across short distances (on the order of a few wavelengths) or brief periods of time (of the order of seconds) [12].

The instantaneously detected signal strength may vary when the mobile moves a short distance, causing a quick fading. Energy components that travel through various paths from the transmitter to the receiver contribute to this impact. These energy constituents can mix productively one moment and destructively the next because their phases are random. The received signal strength can vary substantially (up to 30 or 40 dB) and the phase combination type can change if the mobile travels a very short distance (fraction of wavelengths).

The average received signal power will drop as the mobile gets further away from the transmitter (large-scale models). The track of the distances travelled is typically 5 to 40 times the wavelength. This corresponds to a measuring track of 1 m to 10 m for wireless communication networks operating in the 850 MHz to 2 GHz range [12].

For a specific scenario in a communication system, large-scale and small-scale fading are shown in Figure 1-1. The signal fades quickly as the receiver moves over short distances, but the average signal level varies gradually as the receiver moves over longer distances [10].

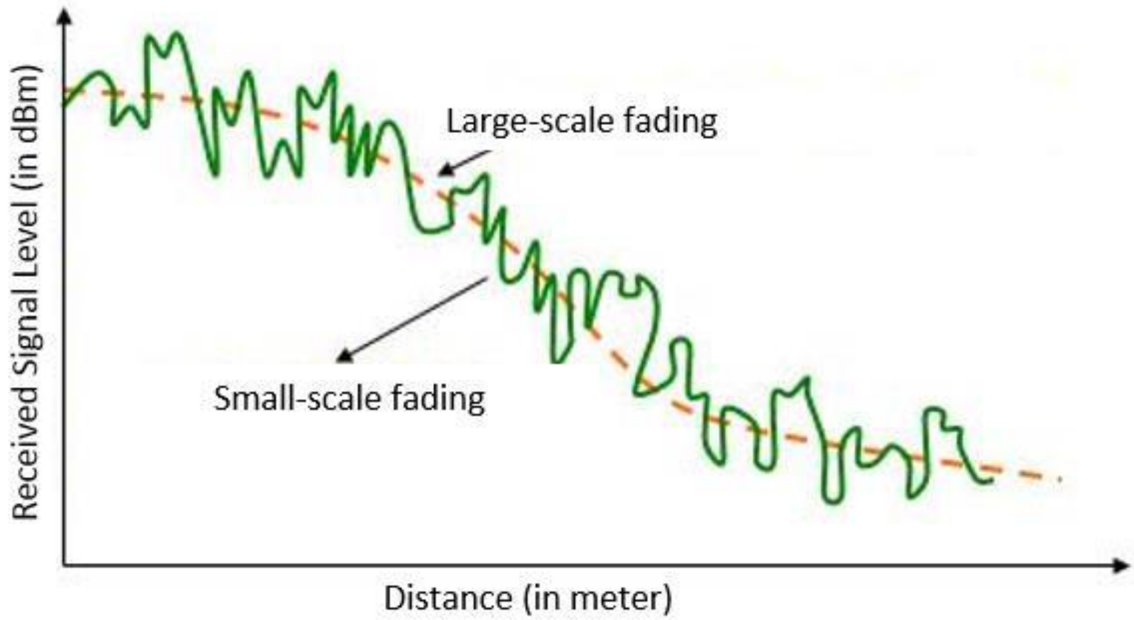

Figure 1-1. Large-scale and small-scale fading effects [10].

1.3 Path Loss and Signal Level Prediction

The path loss is a model for the power density reduction that occurs when a signal travels from one place to another through a particular medium. The primary element that must be taken into account while designing, analyzing, and optimizing wireless communication networks is path loss. The effects of free space loss, reflection, absorption, diffraction, and refraction lead to path loss. As they control how the parts of the propagating signal fields interact with one another. The propagation environment and operating frequency have a direct influence on the path loss [13].

The signal travels from the transmitter to the receiver in free space, taking the form of a sphere with an expanding radius, which causes the wave front to widen, causing the free space losses.

The signal experiences absorption losses when it enters an opaque material. When the wave is impeded by an object's edge, diffraction losses occur. Refraction and reflection alter the signal path, which indirectly reduces signal strength. Adestructive combination may happen at the site of reception if the various components are out of phase.

Prediction is the common name for the path loss calculation. Only straightforward situations, like the empty space, allow for exact prediction. In a real-world setting, one of the following techniques [14] is used to estimate the path loss:

- Empirical approaches (statistical): They are based on measurements made in the field of the average signal strength over the distances traveled.
- Deterministic methods: They are based on the physical principles governing wave propagation.

The statistical approaches are less precise than the deterministic methods, but the deterministic methods demand more complex computations and a highly precise and thorough description of every object in the propagation space.

Since it is taken into account in all situations, including LOS, NLOS, and partial LOS propagation contexts, free-space propagation is an essential part of propagation models. Free space takes into account air as well as vacuums. Almost all wireless communication networks are located close to the earth's surface, so it is important to take into account how these elements interact with one another.

The following two methods can be used to compute the free-space propagation:

- The path loss along the path from transmitter to receiver.
- The strength of the electric field at the receiver in relation to a sending site.

It is possible to express the first strategy, which is to determine the path loss between the transmitter and the receiver, as in Eq.(1-1) [15]:

$$\textbf{Free space path loss} = \mathbf{Lf} = \left(\frac{\lambda}{4\pi d}\right)^2 \ \ldots\ldots\ 1\text{-}1$$

Where:

λ is the propagating signal wavelength in meters.

d is the distance between the transmitter and the receiver in meters.

Equation (1-1) can be re-written to get losses in decibel (dB) units as in Eq.(1-2) [16]:

$$\mathbf{Lf = 32.44 - 10logG_T - 10logG_R + 20\,Log\,f + 20\,Log\,d} \quad \ldots\ldots\ 1\text{-}2$$

Where:

f is the propagating signal frequency in MHz.

d is the distance between the transmitter and the receiver in kilometer.

By putting a radiating source in the center of a sphere, one may determine the strength of the electric field at the receiver in relation to a transmitting site. The surface of the sphere must be penetrated by the total transmitted power P_T (measured in Watts). The average power density S_{av} of the power at distance d travelling through the area is equal to $P_T/4\pi d^2$ if the sphere's surface area is $4\pi d^2$. This is how the free-space field strength can be expressed as in Eq.(1-3) [17]:

$$\mathbf{E} = \sqrt{\eta_o S_{av}} = \frac{1}{d}\sqrt{\frac{\eta_o P_T}{4\pi}} \ \ldots\ldots\ 1\text{-}3$$

Where:

ηo is the free-space impedance in Ohm.

d is the distance between the transmitter and the receiver in meter.

In terms of one microvolt per meter ($dB\mu_{V/m}$), the field strength can be stated as in Eq.(1-4) [17]:

$$\mathbf{E = 74.77 + 10\ Log\ P_T - 20\ Log\ d} \qquad \text{..... 1-4}$$

Where:

d is the distance between the transmitter and the receiver in kilometer.

The field strength in Equation (1-4) does not depend on the signal frequency as in Eq.(1-2).

1.4 Main Propagation Mechanisms

1.4.1 Reflection

The phenomenon of reflection occurs when a ray is incident on a surface has a dimensions larger than the length of the incident signal. The incident signal is reflected at an angle equal to the angle of incidence. The reflected wave fields are linked to the incident wave fields using a matrix known as the reflection coefficient in order to fully characterize the wave field in terms of polarimetry. The most widely used term for reflection is the Fresnel reflection coefficient, which can be used to analyze the boundary between two substances, such as concrete and air. The incident wave field, wavelength, permittivity, conductivity, and polarization of each medium all affect the Fresnel reflection coefficient. The formulas for the Fresnel reflection coefficient are commonly utilized in ray tracing software applications [18].

1.4.2 Diffraction

In ray theory, diffraction is the phenomena that explains the change from a bright area to a shadowy region behind a building's corner or over its roof [19] . Even if the teceived power by the mobile device gradually decreases as it moves closer into the shadowy areas, the device will sometimes make and receive calls [15].

1.4.3 Scattering

Scattering refers to the falling of a signal on a rough surface and then travels in several directions in a three dimentions space. Energy scattering causes a decrease in the level of energy reflected in the specular direction. By lowering the reflection coefficient, the Raleigh theory provides an explanation for this phenomena. A factor smaller than one is multiplied by the reflection coefficient; this factor declines exponentially and is dependent on the surface roughness standard deviation [20].

1.4.4 Penetration and Absorption

The process of absorption by trees and the human body is challenging to quantify accurately. Studies on the reduction of penetration due to construction barriers show that the process varies widely depending on the specific situation. In mobile propagation models, the absorption caused by atmospheric effects is often ignored [19].

1.5 Propagation Models

1.5.1 Introduction

For the design and optimization of wireless networks, propagation models are essential tools. When a signal travels from the transmitter to the receiver, a propagation model can predict its strength. If the receiver is not receiving the signal above the required levels of sensitivity, bit error rate (BER), signal to noise ratio (SNR), and energy per bit to interference ratio (E_b/I_o), the wireless network's performance will be significantly damaged [21]. For the wireless network to operate at its best, the propagation model's job is to anticipate the signal strength and assess if it complies with the receiver's design requirements. The network can be rebuilt and optimized to achieve the goal if performance is below optimal. The classes of propagation models are examined in this section.

Each class's characteristics, benefits, and drawbacks are studied. The most popular propagation models are also discussed along with their benefits and drawbacks.

1.5.2 Classification of Propagation Models

The creation of propagation models received a lot of attention because of their significance in the planning and optimization of wireless network systems. Following are the three basic types of propagation models that have been identified [16]:

- ❖ Theoretical
- ❖ Empirical (statistical) model.
- ❖ Sites-specific (deterministic) model.

The following will go into detail about these types of classes.

1.5.2.1 Theoretical Models

Theories on the behavior of signal propagation form the basis for theoretical models. Physical laws that control signal propagation are used instead of the specifics of the propagation environment. The analysis of wireless communication networks can be done using theoretical models in a wide range of conditions. However, they are not suited for wireless network design and optimization since the specifics of the propagation environment are not taken into account. The behavior of propagating signals is thus governed by simple mathematical relations, which provide the basis for theoretical models class. The examples of this class are in references [22] - [23]. In these examples, it is assumed that the signals being received are a collection of scattered waves. The propagation channel spectrum causes the first and second order fading envelopes. The fact that there is no way to relate the propagation environment in the model formula means that the theoretical models cannot be utilized to mimic a real propagation environment at all.

These factors make theoretical models less common than other models in wireless network design and optimization. Figure 1-2 displays an example of the behavior of a theoretical model.

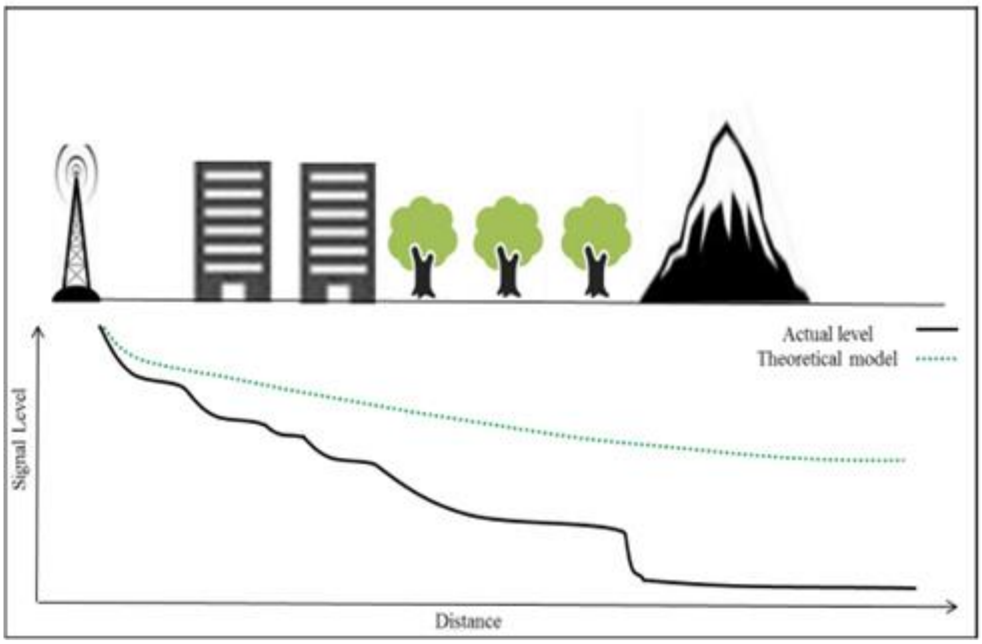

Figure 1-2. An example of theoretical model [15].

1.5.2.2 Empirical Models

The signal level is measured in actual propagation environments for the use of empirical or statistical models, and then mathematical equations are derived from the measurement data (curve fitting). In order to estimate signal level, the resulting mathematical equations are utilized to predict the signal propagation losses in the same or similar environments. In NLOS situations, empirical models are particularly useful for design and optimization.

The empirical propagation models' measurements provide its basis. A measurements are created by measuring the field signal strength with a transmitter at a given location. The measurements can also be performed in labs. The empirical models are frequently employed in the design and optimization of wireless network systems due to their simplicity. The wireless network operators would need to perform periodic measurements to gather signal strength and quality data if they decide to use empirical models for design and optimization. The employed empirical model is then tuned using the measurements [15].

Figure 1-3 displays instances of how the empirical models behave. The models included in the following subsection are those that have been suggested or are now being widely utilized for designing and optimizing wireless networks.

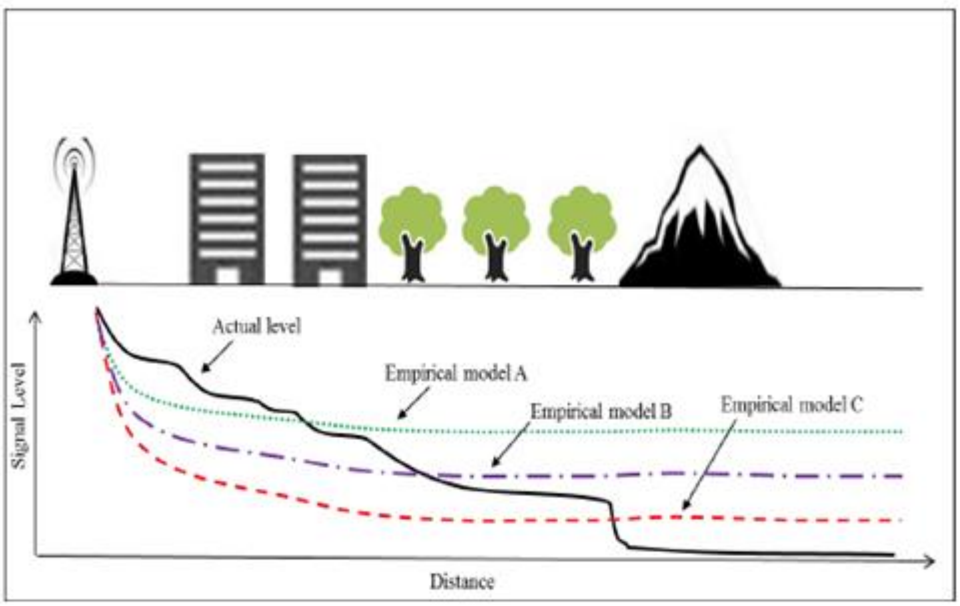

Figure 1-3. Examples of the behaviour of the empirical models [15].

1.5.2.2.1 Okumura Model

For coverage modeling and prediction in urban settings, Okumura's propagation model is frequently employed [5]. It was created to operate between 1 km and 100 km away at frequencies between 150 MHz and 1920 MHz. It is reasonable to assume that the base station's antenna will be between 30 and 1000 meters high.

In order to determine the path loss relative to free space path loss in urban areas in a relatively flat terrain with antenna heights of 3 m and 200 m for the mobile station (h_m) and base station (h_b), respectively, Okumura created a series of curves using the curve fitting approach. Intensive field measurement data using vertical omnidirectional antennas for the base and mobile stations were used to perform the curve fitting. The results are then presented as a function of frequency and distance, with frequency and distance ranges of 100 to 1920 MHz and 1 to 100 km, respectively. By adding the free space losses and the value of the function A(f,d) derived from the curves in Figure 1-4, it is possible to calculate the anticipated path loss between the base station and any point of interest.

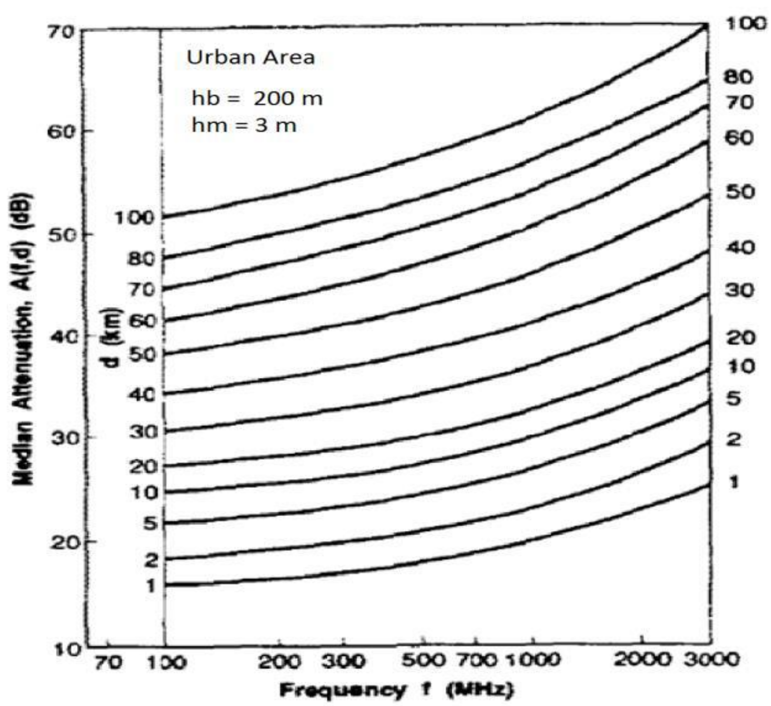

Figure 1-4. A(f,d) Median attenuation relative to free space [5].

To determine the final losses, an adjustment factor based on the terrain type should be included. The Okumura model's path loss can be represented as in Eq.(1-5) [5]:

$$\mathbf{L(dB) = L_f + A(f,d) - G_{hm} - G_{hb} - G_{area}} \quad \text{..... 1-5}$$

Where:

L is the average path loss experienced by the transmitted signal measured in dB.

L_f is the path loss due to free space.

A(f,d) is the average attenuation function with respect to free space obtained from Figure 1-4.

G_{hm} and G_{hb} are the mobile and base station antenna height gains, respectively. G_{area} is a gain related to environment type.

It should be highlighted that the antenna height gains are functions of height only are not related to antenna patterns. It was found that G_{hb} changes with a rate of 20 dB/decade and G_{hm} changes with a rate of 10 dB/decade for antenna heights less than 3 m. Thus G_{hb} and G_{hm} can be expressed as as in Eqs.(1-6), (1-7) and (1-8) [16]:

$$\mathbf{G_{hb} = 20Log\left(\frac{h_b}{200}\right) 1000\ m > hb > 30} \quad \text{..... 1-6}$$

$$\mathbf{G_{hm} = 10Log\left(\frac{h_m}{3}\right) hm \leq 3\ m} \quad \text{..... 1-7}$$

$$\mathbf{G_{hm} = 20Log(\frac{h_m}{3})\ 10\ m > hm > 3} \quad \text{..... 1-8}$$

Where:

h_b is the effective base station antenna height in meter.

h_m is the effective mobile antenna height in meter.

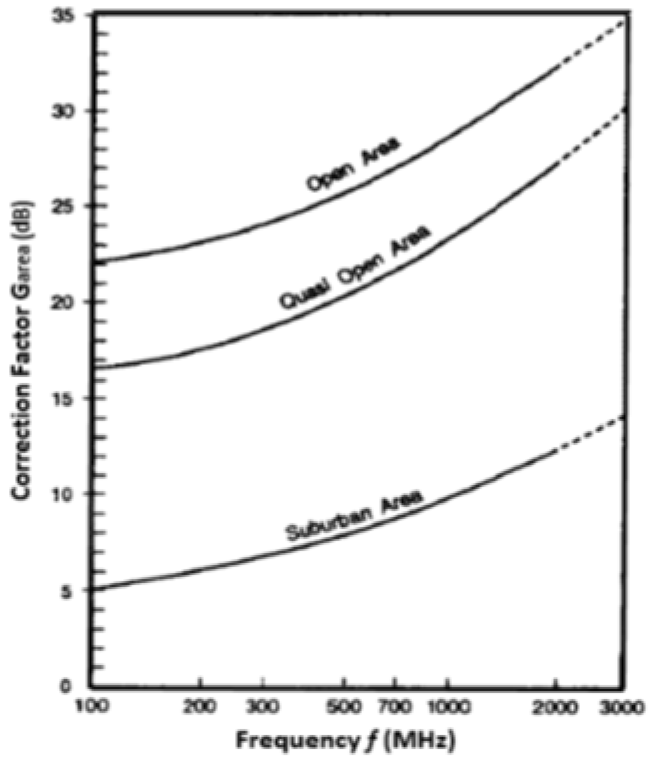

Figure 1-5. The correction factor Garea for different terrain types [5].

Additionally, modifications can be made to Okumura's model by adjusting parameters relating to a particular terrain type, such as the height of the ground slope and the ripple of the building height. The corrective factors can be included in the model once these parameters have been collected.

Okumura's model is totally reliant on the field measurements and is unable to identify the cause of the losses. To find values outside of the field measurement range, the generated curves can be extrapolated, however the accuracy of the extrapolation depends on the type of propagation environment and the smoothness of the curves [5].

One of the simplest and most accurate models for predicting coverage for early cellular networks is the Okumura's model. This approach became a standard for the design and optimization modern networks in Japan because of its practicality. This model's major drawback is that it responds inaccurately to fast fluctuations in the terrain; as a result, it is more accurate in rural terrain than in urban and suburban terrain.

1.5.2.2.2 Hata-Okumura Model

The Okumura propagation model is the foundation of the Hata-Okumura model. In order to narrow the difference between the measured and predicted signal strength at various propagation environments, this model added correction parameters that the Okumura model did not include. The frequency range covered by the Hata-Okumura model is 150 MHz to 1500 MHz. The following are the possible expressions for the urban area formula for the median path loss as in Eq.(1-9) [24]:

$$\mathbf{L_{urban} = 69.55 + 26.16\, Log\, f - 13.82\, Log\, \boldsymbol{h_b} - a(h_{\boldsymbol{m}}) + (44.9 - 6.55 Log\, h_{\boldsymbol{b}}) Log\, d} \quad \text{..... 1-9}$$

Where:

$a(h_m)$ is a correction factor related to the effective height of the mobile antenna and it is also a function of the coverage area.

d is the sepration distance between the base station and the mobile (in km).

The h_b and h_m range from 30 to 200 m and from 1 to 10 m, respectively.

The following [18] is how to find the $a(h_m)$ for a small or medium-sized city as in Eq.(1-10):

$$\mathbf{a(h_m) = (1.1\, Log\, f - 0.7)h_m - (1.56\, Log\, f - 0.8)} \quad \text{..... 1-10}$$

And for a city with the large area it is given as in Eqs.(1-11) and (1-12):

$$\mathbf{a(h_m) = 8.29(Log\, 1.54\, h_m)^2 - 1.1\, dB\; for\; f\; \leq\; 4300\, MHz} \quad \text{..... 1-11}$$

$$\mathbf{a(h_m) = 3.2(Log\, 11.75\, h_m)^2 - 4.97\, dB\; for\; f\; \geq\; 4300\, MHz} \quad \text{..... 1-12}$$

The Hata-Okumura path loss model in equ.(1-5) can be modified to obtain the average path loss in suburban area as follows as in Eq.(1-13) [24]:

$$\mathbf{L_{suburban} = L_{urban} - 2[Log\frac{f}{28}]^2 - 5.4} \qquad \text{..... 1-13}$$

For rural areas path loss, Equation (2.5) can be modified as in Eq.(1-14) [24]:

$$\mathbf{L_{rural} = L_{urban} - 4.78(Logf)^2 + 18.33Logf - 40.98} \qquad \text{..... 1-14}$$

Hata-Okumura model does not contain any path-specific correlations, in contrast to Okumura model, however the prior formulas still have practical value. If the distance d is more than 1 km, the Hata-Okumura model's offer prediction accuracy is comparable to that of the Okumura model. Therefore, the Hata-Okumura model is a great choice for wireless networks with large cell radius, but not for those with cell radius of less than 1 km.

The Hata-Okumura model had many modifications in order to be adaptable to various propagation conditions, like as those used in [22]. Although the results were positive, the essential field measurement requirements are the major drawback of such process.

1.5.2.2.3 COST 231-Hata Mode

The Okumura and Hata-Okumura models are a basis of the COST 231-Hata model. Other correction factors are offered by this model for use in urban, suburban, and open (rural) regions. For urban locations, the basic path loss equation is as in Eq.(1-15) [25]:

$$\mathbf{L_{urban} = 46.3 + 33.9\ Log\ f - 13.82\ Log\ h_b - \alpha(h_m) + (44.9 - 6.55\ Logh_b)Log\ d + C_M)} \qquad \text{..... 1-15}$$

$$\mathbf{\alpha(h_m) = (1.1\ Log\ f - 0.7)h_m - (1.56\ Log\ f - 0.8)} \qquad \text{..... 1-16}$$

Where:

C_M is found as follows:

C_M = 0 dB for suburban areas with medium tree density and rural areas.

C_M = 3 dB for urban and dense urban areas.

The Okumura and Hata-Okumura propagation models and the COST-231 Hata propagation model both have limitations for application in the design and optimization of wireless networks, but because of their simplicity, they are widely used for general design.

1.5.2.3 Site-Specific Models

The site-specific propagation models were developed using the electromagnetic wave theory. Unlike the class of empirical models, site-specific propagation models rely on

information and the details of the propagation environment and use physical mechanisms of propagation to estimate signal propagation losses instead of field measurements.

The design of fixed wireless communication systems is widely for this class of propagation models. In the past few decades, point-to-point wireless networks have been designed utilizing the easy formula for free space path loss and taking consideration any simple reflections over water surfaces that may be in the link's path [16] and [26]. The most important factor in designing such networks was the mix of free-space path loss, multipath fading, and rain modeling. To provide an accurate estimate of signal strength, the terrain databases that provide elevations, clutter heights, and rain rates were all employed in the design process. These connections have been made over lengthy distances of up to tens of kilometers.

All site-specific models consist mainly of the free-space propagation mechanism. The ways that the various site-specific models approach the terrain database, clutter reflections, building penetration, and foliage obstruction attenuation are the key areas where they diverge from one another. Over the past few years, many methods to handle these factors have been developed and proposed. The field measurements were used as the basis for these models' validations. Site-specific models are used by regulators like the FCC in the US because of the high accuracy they provide [15].

The exact computation of electromagnetic wave propagation might theoretically be done by resolving Maxwell's equations. The drawback of site-specific propagation models ,such as Ray-Tracing based approaches, is that they require very complex mathematical calculations and extremely powerful computers.

Geographic Information System (GIS) databases have increased enormously in the last decades, along with the computational and visualization capabilities of computers. Engineers were moved by this important development to design more detailed prediction models that interact with the propagation environment and lead to Ray-Tracing based propagation models. Due to their accuracy, Ray-Tracing techniques have taken plenty of interest. The biggest problem with Ray-Tracing models is how long it takes to compute the signal level estimate. Although Ray-Tracing computation times have decreased recently due to faster processors, it is still mainly a research tool rather than a modeling technique for the design and optimization of the wireless network [27]. Other site-specific models, such as the image method model [23] and Finite-Difference Time-Domain (FDTD) [28], are accurate, but their application is limited by the huge computation and time requirements for small size areas. An example of site-specific model behaviour is presented in Figure 1-6.

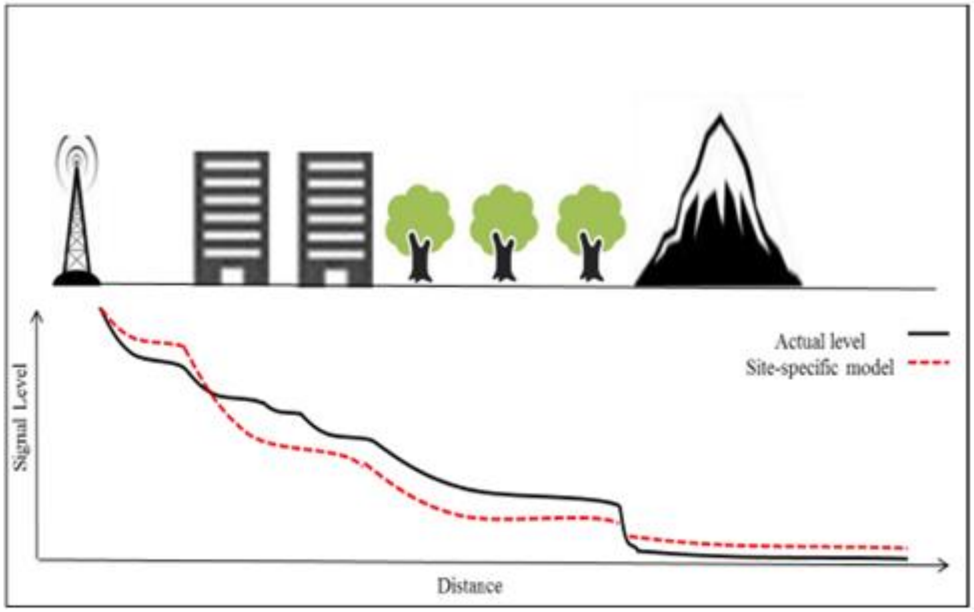

Figure 1-6. An example of site-specific model behavior [15].

1.6 Thesis Aim

This thesis aims to design a mathematical model to predict the received signal strength in mobile communications for 3G and 4G in Amara city. However, there are a variety of models that can be used to predict the power of the signal, such as Hata and COST23 but, these models do not give an accurate prediction of the received signal strength in Amara city.

1.7 Thesis Layout

- The first chapter presents an introduction and includes general introduction to radio signal propagation prediction, radio wave propagation, path loss and signal level prediction, main propagation mechanisms, propagation models, thesis aim, and thesis layout.
- The second chapter presents a literature review of radio signal propagation prediction.
- The third chapter presents the methodology of this thesis.
- The fourth chapter presents the results of this thesis and discusses these results.

- The fifth chapter presents the conclusions of this thesis and recomindations to future researchers.

Chapter Two : LITERATURE REVIEW

2.1 Introduction

This chapter provides an overview of propagation prediction models used for mobile wireless communication systems between 2018 and 2023. It briefly explains classic empirical models, followed by deterministic propagation models developed using ray tracing with deep and machine learning techniques. It also reviews recent studies aimed at improving the computational efficiency and accuracy of propagation prediction models and provides an overview of traditional statistical models. Additionally, it describes new techniques in propagation prediction.

2.2 The Okumura-Hata model, the COST 231 Walfish-Ikegami (COST-WI), and the COST-231 Hata model

The simulation of radio propagation for LoRaWAN at 868 MHz in an urban setting has been performed using 3 models - the Okumura-Hata, the COST-WI, and the COST-231 Hata models in the NS3 [29]. LoRaWAN employed 868 MHz as its radio frequency. The validity and reliability of the empirical models are evaluated by comparing the expected RSS values with real measurements taken in Glasgow when used for LoRaWAN network planning and prediction(see Figure 2-1).

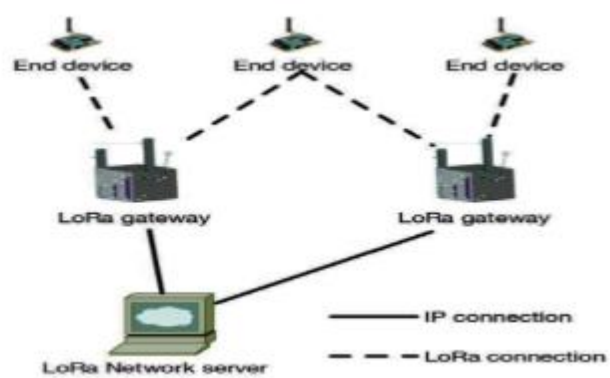

Figure 2-1. LoRaWAN Network Architecture [29].

2.3 Machine Learning - based Propagation Prediction Methods

The effectiveness of the Extreme Learning Machine (ELM) algorithm for creating a precise model for path loss prediction for outdoor propagation scenarios has been investigated [30] (see Figure 2-2).

A machine learning method that attempts latency prediction in an actual network by utilizing real data from a mobile network on the end user has been proposed [31]. The study considered a massive dataset comprising over 238 million latency measurements from three distinct commercial mobile providers. By compressing the Real Time Text (RTT) values into many bins, the methodology converted the latency prediction problem into a multi-label classification problem.

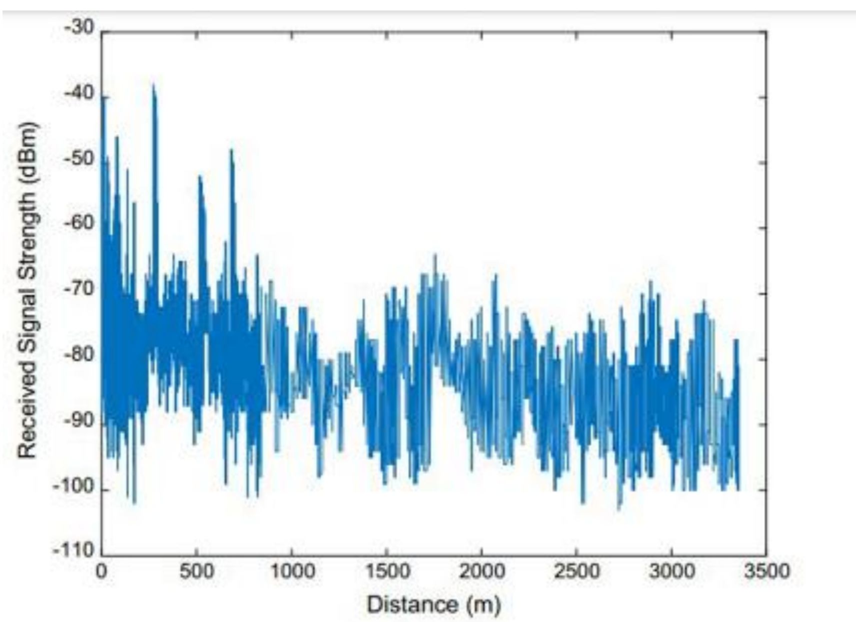

Figure 2-2. Measurement data collected at 1800 MHz [30].

The theory and methodology of Machine Learning (ML-based path loss prediction has been discussed by [32] (see Figure (2-3). Various models were evaluated using measured data, including RF, Support Vector Regression (SVR), and Artificial Neural Network (ANNs). The study reported that these ML-based models perform better than the log-distance model.

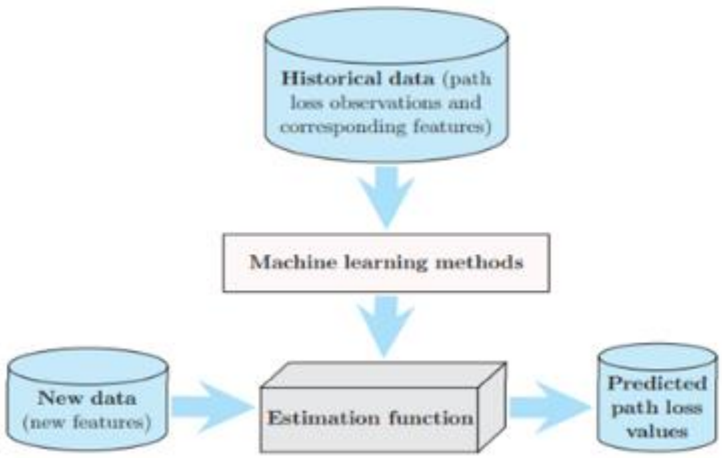

Figure 2-3. Principle of machine-learning-based path loss prediction [32].

A study presented by Nishio (2019) showed that proactive received power prediction is feasible when using spatiotemporal visual sensing data to build dependable mmWave networks [33]. A revolutionary method has been presented by researchers that can forecast the received power time series several hundred milliseconds ahead of the current moment (see Figure 2-4).

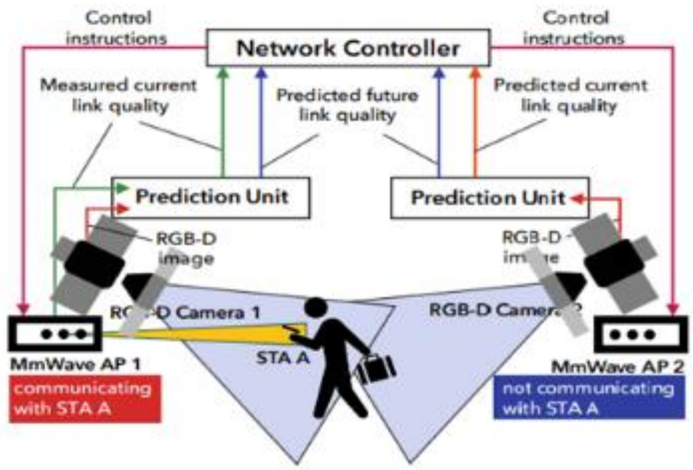

Figure 2-4. System model [33].

A comprehensive analysis has been presented [34] to determine the optimal Neural Network (NN) parameters for path loss prediction in the Very High Frequency (VHF) band. Significant network and geographic data about the mobile device that was received was also acquired, in addition to field measurements conducted to determine the path losses of radio signals broadcast at 189.25 MHz and 479.25 MHz in an urban propagation setting (see Figure 2-5).

A machine learning and building occupancy estimation-based radio propagation prediction approach has been presented [35]. Studies with an emphasis on learning have used building occupancy images and aerial photos as sources of spatial information.

Figure 2-5. RSS measurement set-up [34].

An ML framework for path loss prediction based on three essential techniques - principal component analysis (PCA)-assisted feature selection, Gaussian process-based variance analysis, and multi-dimensional regression based on (ANNs) has been presented [36]. The dataset used to measure path loss usually contains a wide range of features such as antenna height and distance.

The prediction of radio propagation features using an ML-based method called Gradient Boosting has been reported [37]. The model considered building data around the transmitter and a receive site as the features due to their significant impact on radio propagation characteristics. The prediction accuracy may be enhanced from around 10 dB in the traditional method to around 3.3 dB.

A method for received signal strength (RSS) estimation and radio wave propagation modeling based on ML for supplementing the empirical or ray tracing-based models has been proposed [38]. The suggested ML-based model makes use of a pre-identified set of smart predictors, such as transmitter parameters and the geometric and physical properties of the propagation environment to calculate the RSS. The results showed that Deep Neural Networks outperform other ML techniques by offering a prediction accuracy gain of 25 % over the state-of-the-art empirical models, and a prediction time decrease of 12x over ray tracing.

Scholars have suggested that drones, Artificial intelligent (AI), and Internet of Things (IoT) could collectively produce good solutions to some of the issues faced today in smart cities [39]. Drones can travel to places that are dangerous, challenging, or even impassable for people to enter. Drones were just data-gathering machines.

Scholars in [40] employed measured atmospheric factors for the construction of ANN models for RSS computation for 4 VHF broadcast stations. The Levenberg

Marquardt Back Propagation (LMBP) technique was considered for the network training. The MSE calculated by the model ranged from 0.0027 to 0.0043, which is a very low error range. After testing the accuracy of the trained model with various datasets, the obtained results for one dataset in terms of Mean Sequare Error (MSE) was 0.0069, while for another, it was 0.0040.

To overcome these problems, a novel location estimation model suggested [41] which comprises two modules, one for learning to predict, and the other for estimating position in an interior setting through sensor fusion. The results showed that the suggested learning-to-predict model greatly increases prediction accuracy, which provided the confidence to investigate its use further to enhance the functionality of other indoor prediction models.

An ML-based radio propagation model for interior settings analyzed previously [42]. The suggested neural network has a dropout layer that was introduced to randomly disable the network units to increase generalization performance.

Intelligent techniques for connecting the IoT with unmanned aerial vehicles (UAVs) with optimal network connectivity and required quality of service (QoS) have been suggested [43]. Adaptive data transmission is made possible by the prediction of signal strength and fading channel conditions, which improves end users' and devices' quality of experience while using less power for data transmissions.

2.4 Deep Learning- based Propagation Prediction Methods

Deep Channel, a sequence-to-sequence Deep Learning (DL) model based on an encoder-decoder that can predict future variations in wireless signal strength based on historical signal strength data developed by [44]. The researchers studied two distinct iterations of Deep Channel, where in the initial version, Long Short Term

Memory (LSTM) was used as its fundamental cell structure, while the subsequent version uses Gated Recurrent Units (GRU).

A new analytical model that incorporates latency, radio resource waste, call dropping, and signaling overhead for the holistic handover (HO) cost evaluation presented has been [45]. The created mathematical model can be applied to various cellular structures (see Figure 2-6).

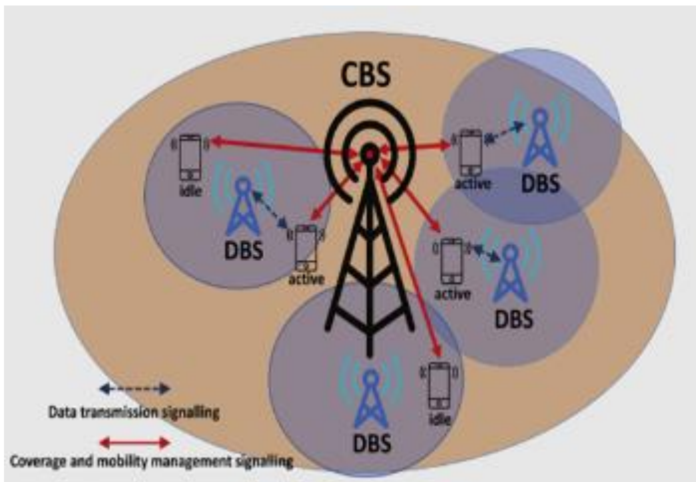

Figure 2-6. Sample CDSA architecture [45].

The study by [46] first showed that the ideal mmWave beam and blockage status can be efficiently predicted from the sub-6 GHz channel using mapping functions as long as certain provisions are made.

Researchers have demonstrated the use of a DNN for predicting radio propagation [47]. The DNN can work with non-linear functions, so, there is no need to derive complex functions.

The researchers in [48] found dramatically increased performance when compared to conventional models following the use of a novel approach for radio propagation modeling using DNNs.

A novel DL-based path loss prediction model that relies on the top-view image of the receiver position for implicit extraction of radio propagation properties has been presented [49].

In the study by [50], a channel model developed by DL approaches using satellite images with the assistance of a basic path loss model was benchmarked against traditional channel models. The proposed DL model can improve path loss prediction by ≈ 1 dB & ≈ 4.7 dB for 2630 MHz at unseen locations (see Figure 2-7).

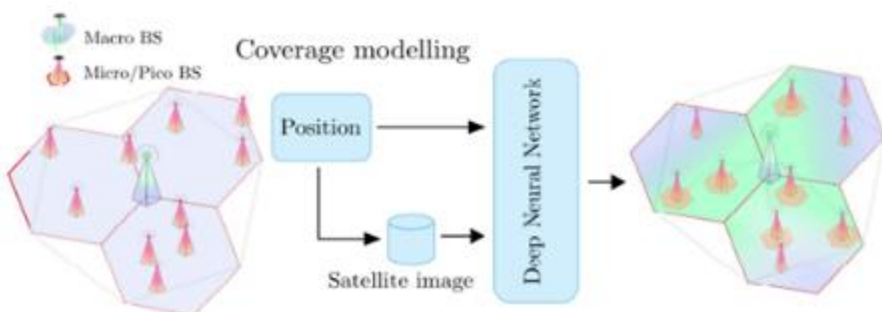

Figure 2-7. Complex channel models are needed for coverage prediction in complex scenarios [50].

The accurate prediction of path loss (PL) requires accurate prediction of the transmitter coverage and optimization of the performance of a wireless network. It is challenging for traditional PL models to keep up with the growing trend of various, time-varying, and huge wireless channels. To accurately predict PL, the most popular MLP neural network in ANN is used in the work reported by [51] (see Figure 2-8).

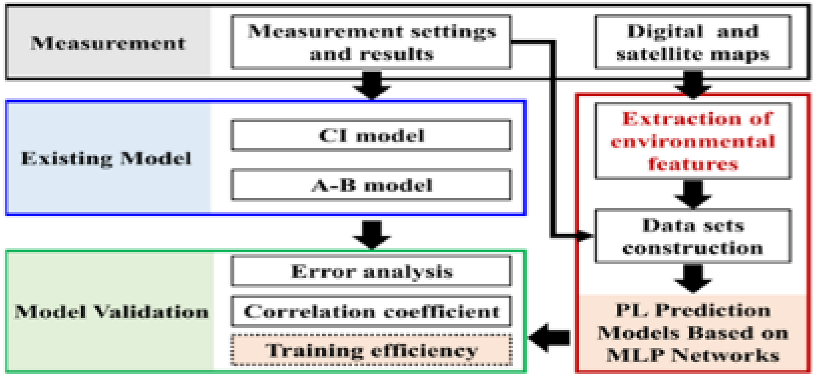

Figure 2-8. The workflow of PL prediction models [51].

Spectrum data learning and solving difficult tasks in 5G and beyond, such as beam selection for initial access (IA) in mmWave broadcast using DL-based algorithms have been presented [52]. Using RSSs from a subset of possible narrow beams, a DNN may forecast, for directional broadcasts, the beam that is ideally slanted to each user equipment (UE).

deep neural networks (DNNs) has been reported [53]; the work relies on a 3D map of the surrounding area and signal strength samples gathered throughout the prediction space to forecast the radio waves' scattering through the environment.

Researchers took into consideration a dataset that includes simulated power for a specific set of transmitter locations at every position in an area. For instance, various ML models, such as NNs, K Nearest Neighbor (KNNs), and Generalized Linear Models (GLMs) have been used to predict the power values for specific transmitter sites [54] (see Figure 2-9).

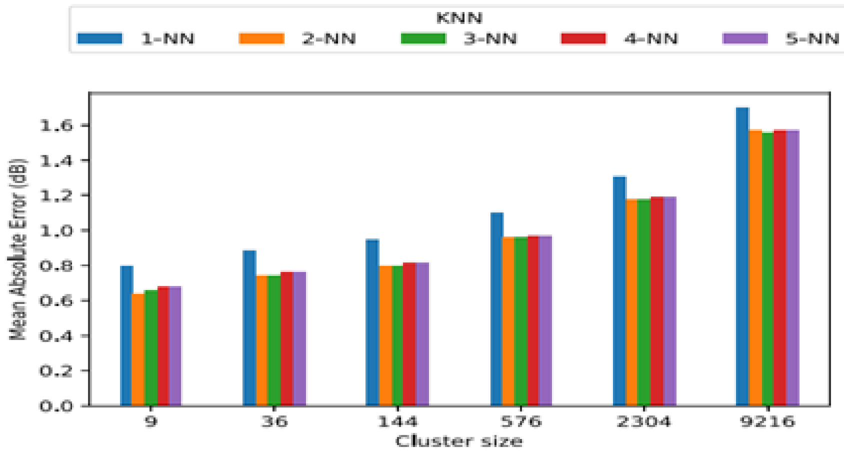

Figure 2-9. hyper parameter search results [54].

A deep learning approach for calculating the propagation path loss on a planar domain from a transmitter site, point x, to any other point y, with high efficiency and high accuracy has been proposed [55].

A costly step in determining the ideal transmitter placement with ray tracing software was accurate radio frequency power prediction in a given geographic area. The researchers in [56] empirically analyzed the viability of DL models to speed up this procedure.

A unique Multilayer Perceptron- Neural Network (MLP-NN-based model for path loss prediction has been reported [57], together with a guided implementation network architecture and a method for hyperparameter tuning based on grid searches. The suggested model is built to approximate path loss between the BS and the mobile station as best as possible.

2.5 Propagation of ad hoc Wireless Local Area

The propagation of ad hoc WLANs operating at 2.4 GHz and 5 GHz, which are commonly employed for near-shore autonomous surface vehicle operations, was studied by [58]. The same physical equipment was used in nearly the same location to collect RSSI data at two different frequencies over land and seawater, as well as two different ground station antenna heights to isolate the marine environment effect. The findings indicate that when moving from over-land to over-seawater, the proposed 2.4 GHz, 2 m antenna height system experienced a 2 to 3 dBm path loss (corresponding to a 25 to 40% reduction in range).

2.6 Ray Tracing - based Propagation Prediction Methods

A 3-D ray tracing (RT) simulation was presented by [59] with a 38 GHz indoor mmW propagation prediction; an additional simulation that was run utilizing the 3-D shooting bouncing ray (SBR) approach was also given. Simulations were performed using the current SBR on a particular layout where the measurement was taken, while the suggested RT approach was also implemented separately (see Figure 2-10). Table 2-1 represents antenna configuration details.

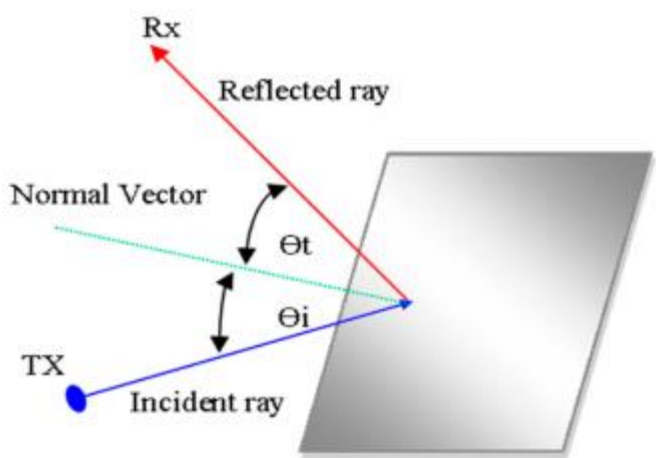

Figure 2-10. Geometric representation of the reflection [59].

Table 2-1. Antenna configuration details [59].

SL.	Item	Properties
I	Gain (dB)	20
II	Frequency range (GHz)	26.5–40.0
III	Beam width (deg.)	18
IV	Waveguide	WR28
V	Material	Cu

VI	Output	A Type: FBP 320, C Type: 2.9 or 2.4 mm-F
VII	Size (mm) W × H × L	A Type: 40.5 × 32 × 70, C Type: 40.5 × 32 × 95
VIII		A Type: 0.05 Around, C type 10 Around

Another study of the 28 GHz indoor radio wave propagation using an effective three-dimensional ray tracing (ETRT) technique presented by [60]. The measurement data was used to validate the ETRT model-based simulation program and the simulation and measurement data showed significant agreement for the path loss and received signal strength indicator. The Measurement setup as in Table 2-2.

Table 2-2. Measurement setup [60] .

SL.	Item	Values
1	Carrier Frequency (GHz)	28
2	Transmit Power (dBm)	25
3	Tx Hom Antenna Gain(dBi)	19.2
4	Rx Omni Antenna Gain(dBi)	3
5	Tx Height(m)	1.5

As suggested by [61], a high-resolution environment model can be better captured using point cloud data (PCD) compared to a conventional geometrical mesh. Hence, PCD is suited for the prediction of mmWave radio channels in a new environment (see Figure 2-11).

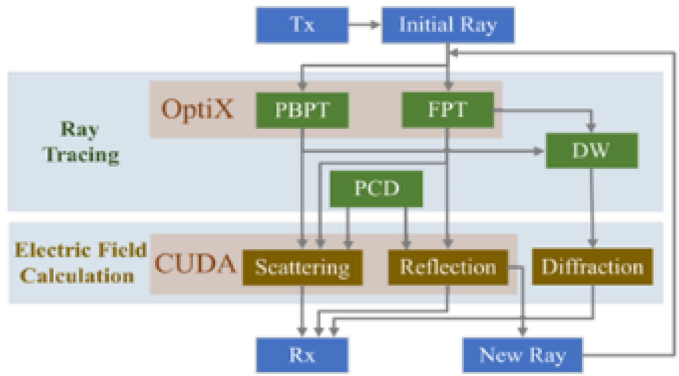

Figure 2-11. Flowchart of GPU-based radio wave propagation prediction [61].

2.7 Wavelet - based Propagation Prediction Methods

A novel approach for predicting spatial electric field strength, called Wavelet- Generalized Regression Neural Network (GRNN) has been proposed [62]; the approach combines wavelet-based decomposition with a GRNN neural network model, which captures important information for robust predictive learning (see Figure 2-12).

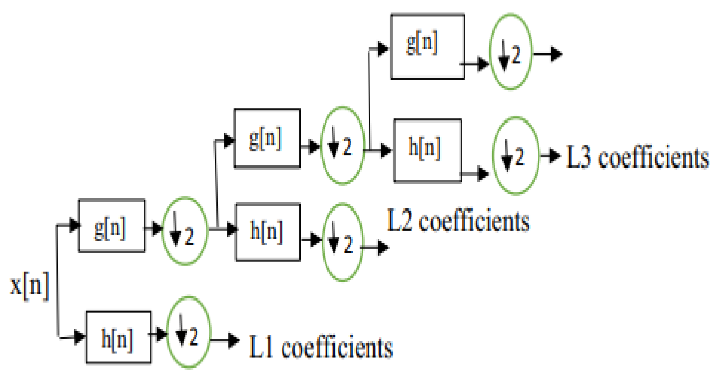

Figure 2-12. Three decomposition level to be used as input to the GRNN [62].

2.8 Random Forests (RFs) - based Propagation Prediction Methods

To enhance signal strength maps acquired from sparse measurements, a prediction framework based on random forests was presented by [63].

2.9 Adaptive Neuro-Fuzzy Inference System (ANFIS)

The development of a path-loss model for accurate estimation of the wireless High-Speed Packet Access (HSPA) network signal in Ibadan, Nigeria, reported in [64]; the model was developed using the ANFIS (see Figure 2-13).

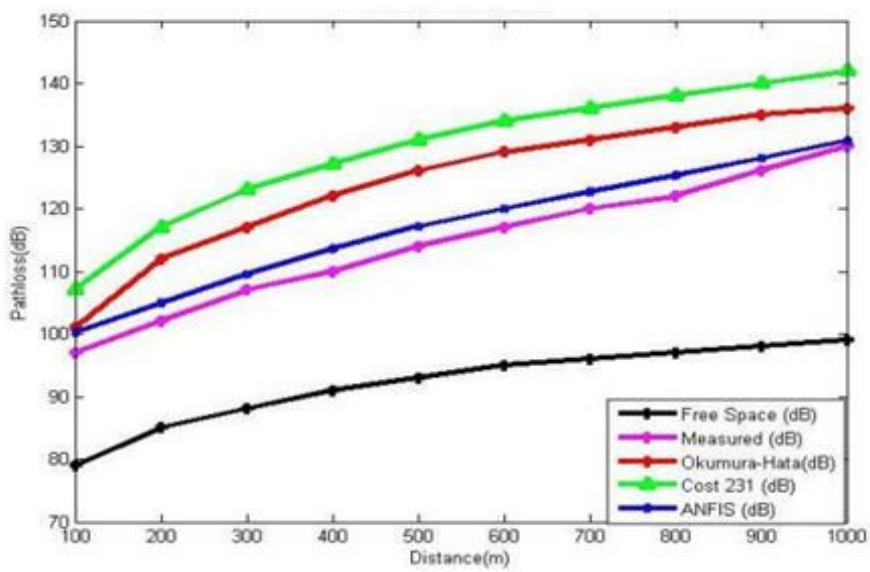

Figure 2-13. Path-loss versus distance for ANFIS [64].

2.10 FDTD and ADI-PE Techniques - based Propagation Prediction Methods

Huang , Xiaoping, Zihao and Yongdong [65] presented a cost-effective hybrid method that combines the Finite-Difference Time-Domain (FDTD) and Alternating Direction-Implicit Parabolic Equation (ADI-PE) techniques for accurate and quick deterministic 3D radio wave propagation forecasts with intricate structures in both far and near-field scenarios, especially in challenging terrains. The study employed a Woodbury-formula-based parallel algorithm to calculate inverse matrices of tridiagonal matrices in a bid to address the inefficiencies of the parallel ADI-PE models.

2.11 ITU Model

For 5G systems and beyond, the precision of rain attenuation prediction is essential for predicting signal strength and link budget for short-range mm-wave terrestrial links. The study by [66] focused on improving the rain attenuation forecast over mmwave frequencies for a short-distance channel (< 1 km).

The researchers [67] conducted a thorough analysis of computational intelligence-based techniques for forecasting and assessing attenuation caused by external causes when designing radio links. Additionally, a modified ML-based intelligent prediction model was used for predicting rain-induced attenuation.

Chapter Three : METHODOLOGY AND PROCEDURES

3.1 Introduction

The goal of this thesis is to design a mathematical model to predict the strength of the signal reaching the recipient in the mobile communications for Misan governorate/ Amarah city. However, there are a variety of models that can be used to predict the power of the signal, such as COST231 and Hata.

In fact, there is a need for a model in case it's applied by the city's communications companies that could be useful in giving sufficient information about the coverage of the transmitters. Therefore, it is useful to know the usefulness of installing such transmitters at designated locations. The mobile communications in the city of architecture use the 2100MHz and 2600MHz frequency for 3G and 4G communications respectively.

Starting from this, 3G and 4G communications were used in the process of measuring and generating the mathematical model.

3.2 Drive Test (DT)

The aim of Drive Test is to measure the signal strength at the reciver .The Drive Test (DT) is wireless network performance assessment from the field using a special program such as TEMS and MapInfo program. To check the wireless network's performance, the operator send an engineer to a certain location. The engineer makes use of a program specially made for measuring. The program measure and record network parameters including signal strength, quality, etc. The DT engineer can also record how the network responds to simulated end user requests for internet access. Since the DT engineer can establish a connection and see whether it drops or fails at handover if he travel from one cell to another, this is also suitable for retain-ability and mobility performance assessments. The GPS integration in the DT test tools allows the engineer to find the issue's exact location within a certain region. The tests are recorded, replayed offline, and examined for network optimization and troubleshooting.

The Drive Test (DT) is a crucial tool for operators to evaluate their network's performance from the end user's perspective. Unlike other methods, DT surveys can identify issues like poor voice quality, slow internet browsing, significant shadowing loss, and out-of-coverage areas. By running regular DT surveys, operators can adjust their networks to achieve high performance and attract more users.

There is a problem with the DT that it requires a significant amount of money and time for its implementation in large areas. Moreover, problems that occur in inaccessible areas cannot be detected. To measure the signal strength of a wireless network (3G Technology), a DT was used. However, the survey could only be conducted over 0.6 km^2 of the total 2 km^2 area, which was the only accessible part of the region. This is the major drawback of DT method.

3.3 Drive Test setup

The measuring equipment used for this project includes TEMS (Test Mobile System) phones connected to a digital computer system running the TEMS investigation tool via a USB hub port. The computer receives the measured data from the TEMS phones and saves it as recorded log files. The log data (signal strength) is then analyzed using MapInfo Professional . MapInfo Professional is a geographic information system (GIS) used for location analysis and mapping see Figure (3-1). Measurements were taken at 4 sites in Amara city for both 3G with 2100MHz and 4G with 2600MHz communications frequencies.

Figure 3-1. Drive Test mechanism.

3.4 The Proposed Model (Misan Model)

The proposed model is an improvement to the Ericson model .Ericson path loss formula as in Eqs. (3-1) (3-2) [68].

$$PL_{\text{ERICSsoN}}\,(dB) = a_0 + a_1\log_{10}(d) + a_2\log_{10}(h_t) + a_3\log_{10}(h_t)\cdot\log_{10}(d) - 3.2\log_{10}(11.75h_r)^2 + g(f) \quad \text{….. 3-1}$$

$$g(f) = 44.49\log(f) - 4.78(\log(f)^2 \quad \text{….. 3-2}$$

a_0= 36.2, a_1= 30.2, a_3= 12.0, a_4= 0.1

The path hoss formula for the proposed model as in Eq.(3-3)

$$P_{loss} = n_o + \mathbf{n_1} * \log(\mathrm{d}) + \mathbf{n_2} * \log(\mathrm{ht}) + \mathbf{n_3} * \log(\mathrm{ht}) - 3.2 * (\log(11.75 * \mathrm{hr}))^2 + 45.1 * \log(\mathrm{f}) \quad \text{….. 3-3}$$

Where:

(ht) is a height of the transmitter antenna .

(hr) is a height of the mobile antenna .

d is the separation distance between the base station and the mobile (in km).

f is the used frequency in MHz.

no = 57, n1=48, n2=17, n3=0.11 for urban area for distance ≥200 m.

no = 40, n1=18, n2=17, n3=0.11 for urban area for distance <200 m.

Figure (3-2) shows procedures of this thesis. The procedures are:

1. Calculation of signal strength using propagation models such as FSPL, Hata, and COST231.

2. Measurement of received signal strength by Drive Test.

3. Calculation of adjustment parameters n_0, n_1, n_2 and n_3 .

4. Calculation of signal strength using the proposed model.

5. Calculation of RMSE for all

models.

6. Comparison between received signal strength produced by propagation models and received signal strength produced by the proposed model.

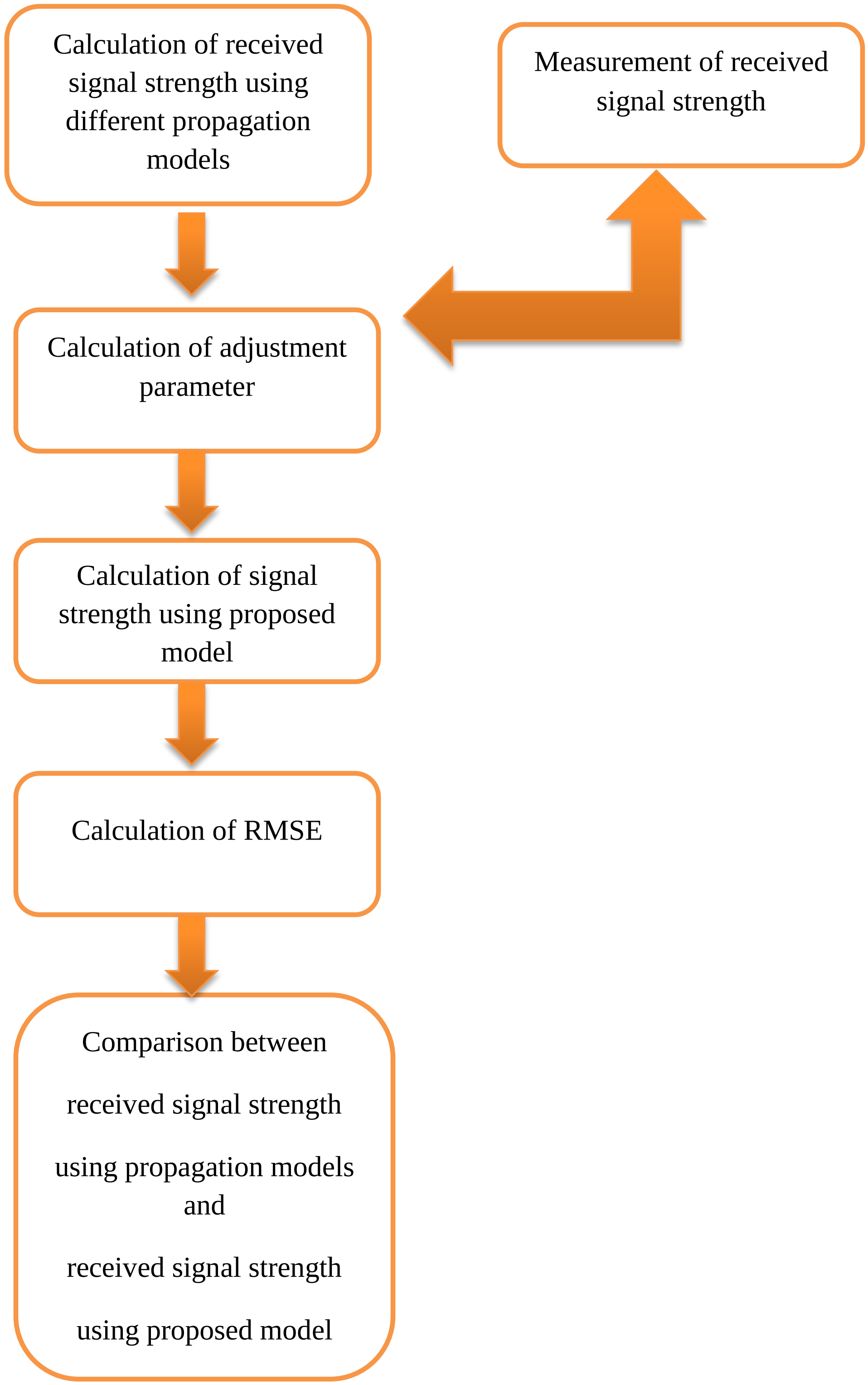

Figure 3-2. Procedures of the thesis.

3.5 Environment of the Model

The investigation is focused on the southern part of Iraq, specifically the Misan governorate and Amarah city, located at latitude 31.837901˚ and longitude 47.142067˚. The thesis collected measurements typical of an urban settlement from four different areas operating at 2100MHz and 2600MHz in the center of Misan.

The measurement takes for 4 sites . These sites coordinates are shown in Table (3-1). The transmitted antenna height (ht) for 4 sites is 21m and mobile antenna height (hr) is 1m.

Table 3-1. Coordinates of sites .

Sites	Coordinates	
	Latitudes	Longitudes
1	31.841105˚	47.144121˚
2	31.868504˚	47.157330˚
3	31.882488˚	47.173051˚
4	31.873121˚	47.144453˚

Figures (3-3) to (3-9) show the location of sites from Google Earth Pro.

Figure 3-3. Site of Misan Governorate from google earth pro.

Figure 3-4. Amarah city from google earth pro.

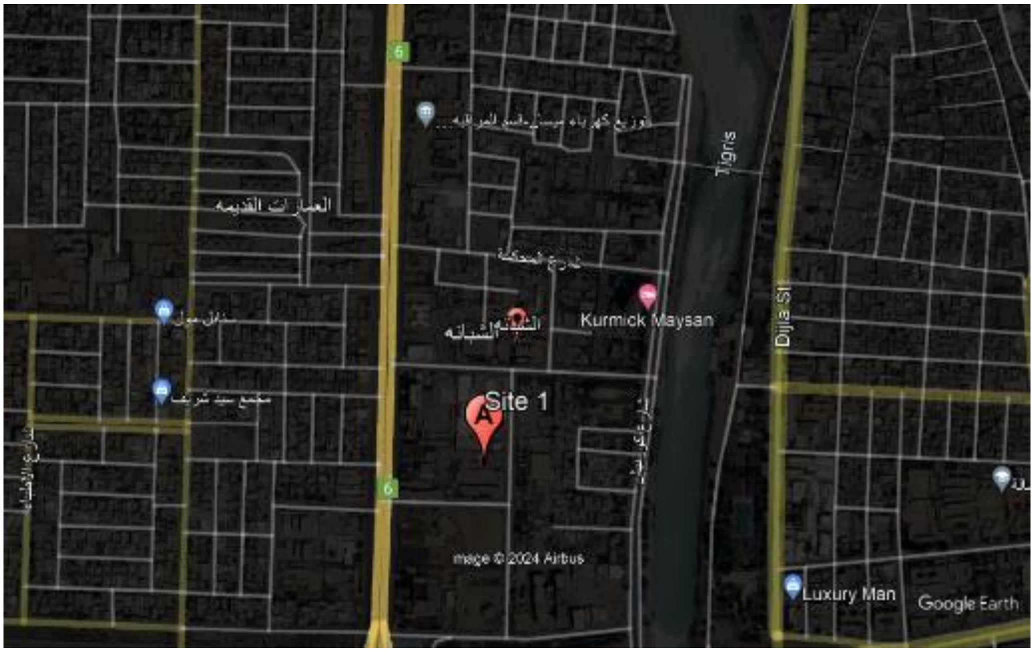

Figure 3-5. Site 1 from google earth pro.

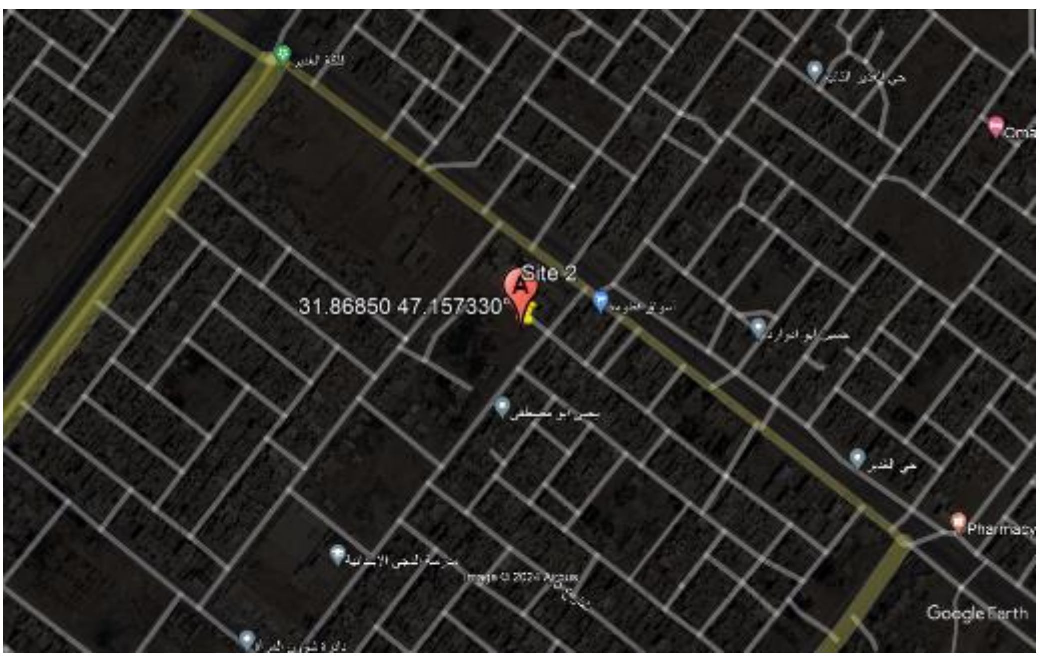

Figure 3-6. Site 2 from google earth pro.

Figure 3-7. Site 3 from google earth pro.

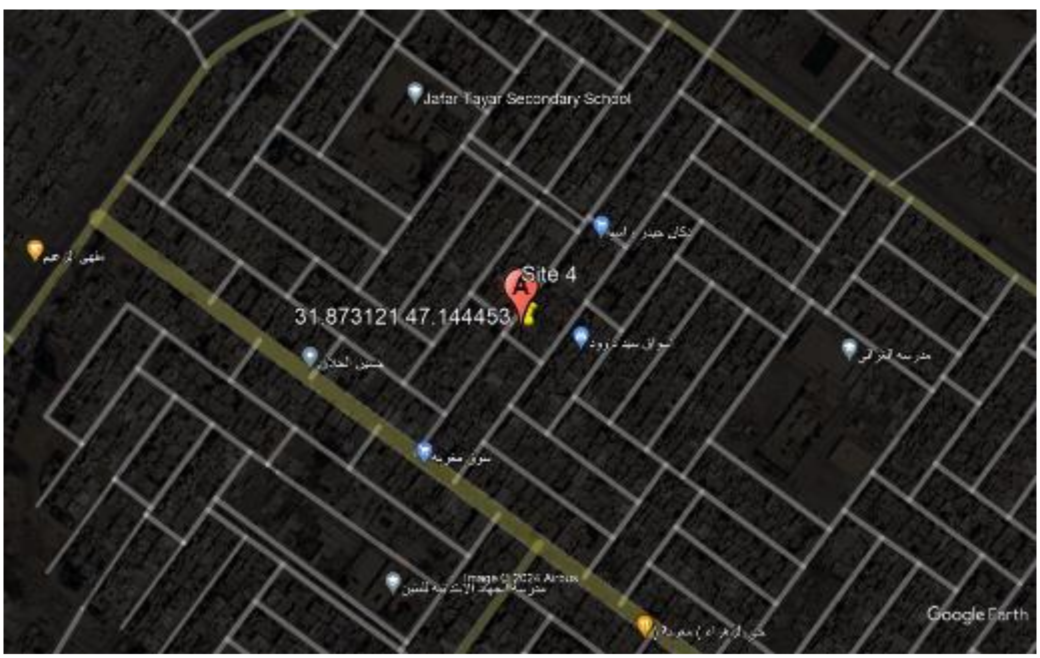

Figure 3-8. Site 4 from google earth pro.

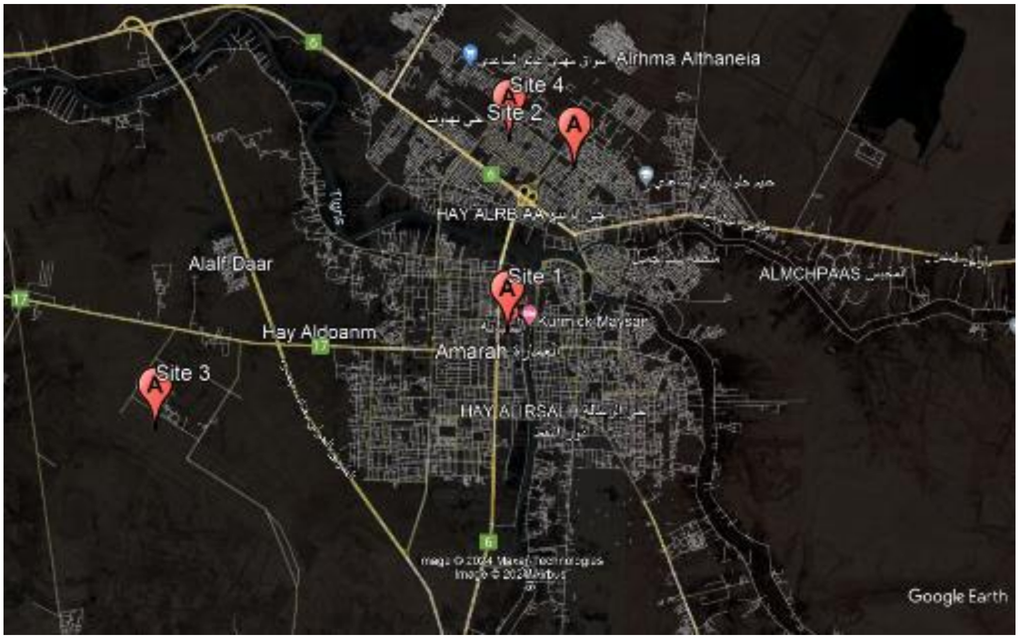

Figure 3-9. All tested sites from google earth pro.

Figure 3-10. UMTS for Site 1.

Figure 3-11.UMTS for Site2.

Figure 3-12. UMTS for Site 3 .

Figures (3-10), (3-11), and (3-13) shows the UMTS for sites. These sites are similar in their climatic environment and differ in population density, number of buildings and their height. Site 3 is less densely populated than other sites.

Figure 3-13. Measurement mechanism for site 2

Figures(3-13) consists of TEMS phone and laptop. The TEMS phone received signal from UMTS. The laptop receives the measured data from the TEMS phone and saves it in the form of recorded log files. MapInfo Professional was then used to analyze these log data.

Chapter Four : RESULTS AND DISCUSSIONS

4.1 Introduction

This chapter verifies the procedures of the proposed method by comparing it with DT. The validation should be completed by using the DT to calculate the Root Mean Square Error (RMSE). Four sites were chosen for the experiments to prove that the proposed model is applicable for urban area.

4.2 Signal Path Loss Calculation for 3G at 2100MHz:

The selected models, including Free Space Path Loss (FSPL), Hata, COST231-Hata, and Misan model, rely on data to predict the mean path loss base on various factors such as environmental areas, distance from the tower, and antenna heights. These models' mathematical equations are incorporated into a MATLAB 2020 computer program specifically designed for the current analytical process. The path loss estimates for the aforementioned prediction models are computed using equations (1-2), (1-9), (1-15), and (3-1). The calculated path loss results are depicted in Figure (4-1) and Table (4-1).

Table 4-1. Signal path loss in different propagation models.

Distance in Meter	Path loss in dB			
	FSPL	Cost231-Hata	Hata	Misan model
40	70.9256	94.2956	88.8317	128.5140
200	84.9050	119.6259	114.1619	139.2188
400	90.9256	130.5351	125.0711	148.4976
600	94.4474	136.9165	131.4526	157.0664

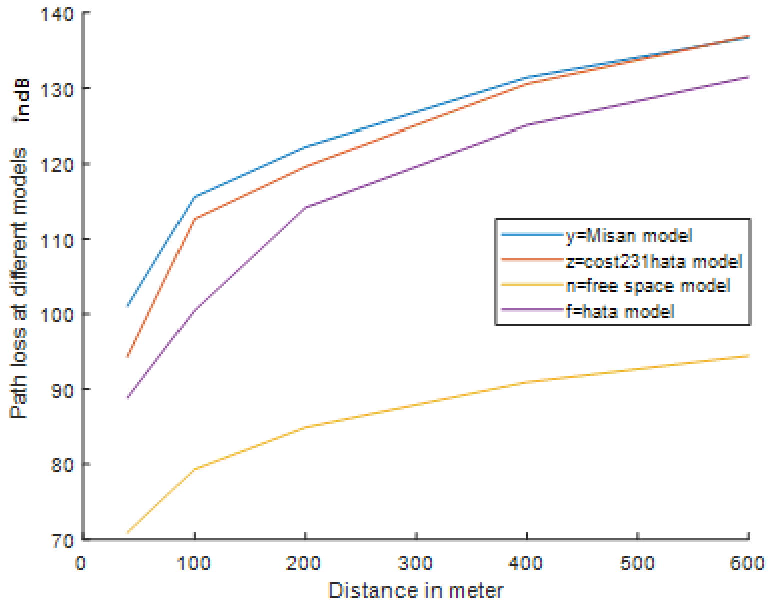

Figure 4-1 Path loss at different models.

The path loss at 2100 MHz is depicted in Figure 4-1. It shows the path loss for transmitted antenna heights of 21 meters and mobile antenna heights of 1.0 meters at distances of 40, 200, 400, and 600 meters between the transmitter and receiver. Additionally, the proposed Misan model is compared with the Hata model, the COST231 model, and the signal strength of the free space model in terms of path loss. Comparing the models reveals that the suggested model has a higher path loss than the other models. However, this will provide signal strength closer to the measured signal strength than other models.

4.3 Signal Strength Calculation for 3G at 2100MHz:

The signal strength represents the power output of a transmitter as measured by a reference antenna located far away from the transmitting antenna. The received signal strength for the Misan model, Hata model, FSPL model, and COST-231 model can be calculated as in Eq.(4-1) [69]:

$$\mathbf{Pr = Pt + Gt + Gr - PL} \qquad \ldots\ldots 4\text{-}1$$

Where

Pr is received signal strength in dBm.

Pt is transmitted power in dBm.

Gt is transmitted antenna gain in dBm.

Gr is received antenna gain in dBm.

PL is total path loss in dBm.

For tested area Gt = Gr = 16dBm and Pt = 42dBm

The signal strength for proposed model is closer to the measured signal strength as in Tables 4-2.

Table 4-2 .Comparison of signal strength in different propagation models at different distance between transmitter and receiver for site 1 .

Distance in meter	Signal Strength in dBm				
	FSPL	Cost231-Hata	Hata	Misan model	Measured signal strength
40	-3.0744	-20.2256	-14.8317	-55.9017	-53
200	-10.9050	-45.6259	-40.1619	-65.2188	-63
400	-16.9256	-56.5351	-51.0711	-75.4976	-74
600	-20.4474	-62.9165	-57.4526	-83.0664	-78

Table 4-3. Comparison of signal strength in different propagation models at different distance between transmitter and receiver for site 2 .

Distance in meter	Signal Strength in dBm				
	FSPL	Cost231-Hata	Hata	Misan model	Measured signal strength
40	-3.0744	-20.2256	-14.8317	-55.9017	-53
200	-10.9050	-45.6259	-40.1619	-65.2188	-63
400	-16.9256	-56.5351	-51.0711	-75.4976	-70
600	-20.4474	-62.9165	-57.4526	-83.0664	-78

Table 4-4. Comparison of signal strength in different propagation models at different distance between transmitter and receiver for site 3 .

Distance in meter	Signal Strength in dBm				
	FSPL	Cost231-Hata	Hata	Misan model	Measured signal strength
40	-3.0744	-20.2256	-14.8317	-55.9017	-60
200	-10.9050	-45.6259	-40.1619	-65.2188	-70
400	-16.9256	-56.5351	-51.0711	-75.4976	-76
600	-20.4474	-62.9165	-57.4526	-83.0664	-78

Table 4-5. Comparison of signal strength in different propagation models at different distance between transmitter and receiver for site 4 .

Distance in meter	Signal Strength in dBm				
	FSPL	Cost231-Hata	Hata	Misan model	Measured signal strength
40	-3.0744	-20.2256	-14.8317	-55.9017	-54
200	-10.9050	-45.6259	-40.1619	-65.2188	-61
400	-16.9256	-56.5351	-51.0711	-75.4976	-69
600	-20.4474	-62.9165	-57.4526	-83.0664	-75

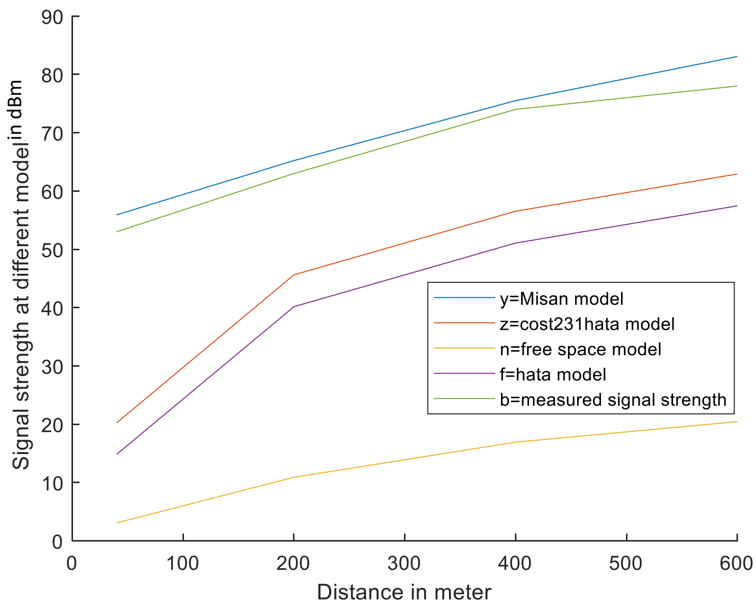

Figure 4-2 Comparison of signal strength at different models in site1.

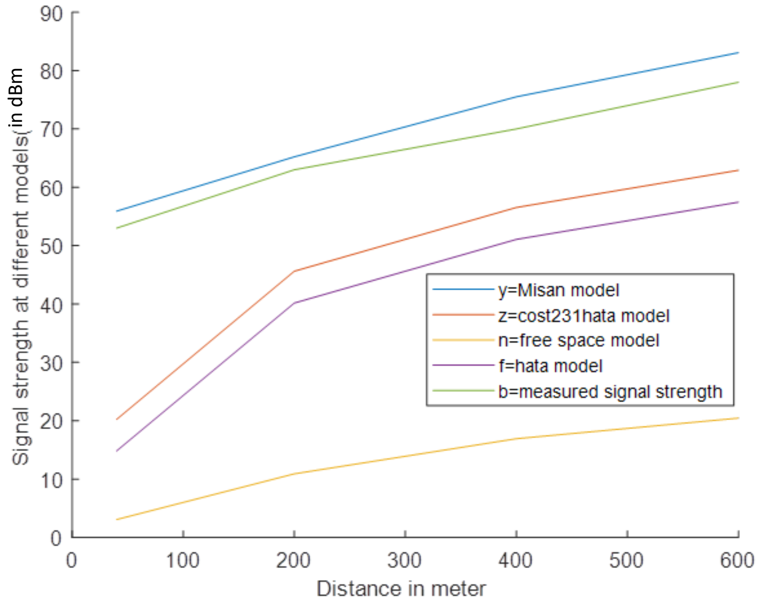

Figure 4-3 Comparison of signal strength at different models in site2.

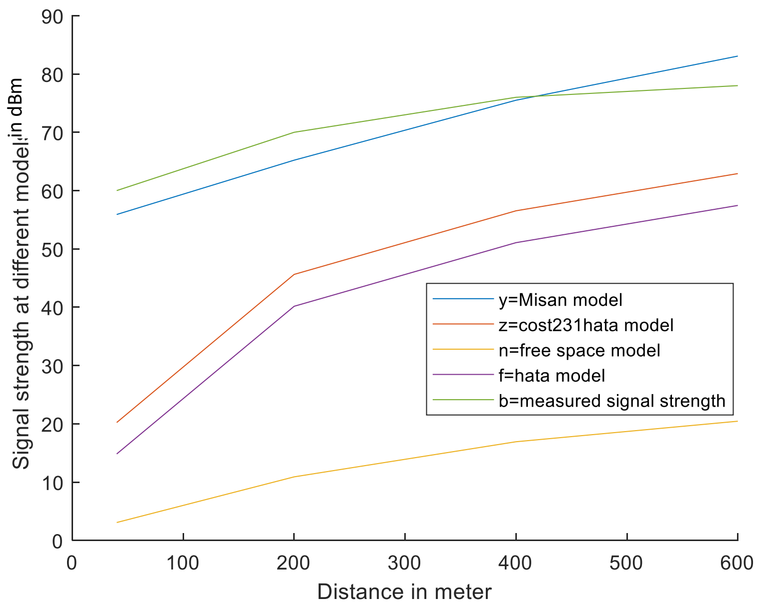

Figure 4-4 Comparison of signal strength at different models in site3.

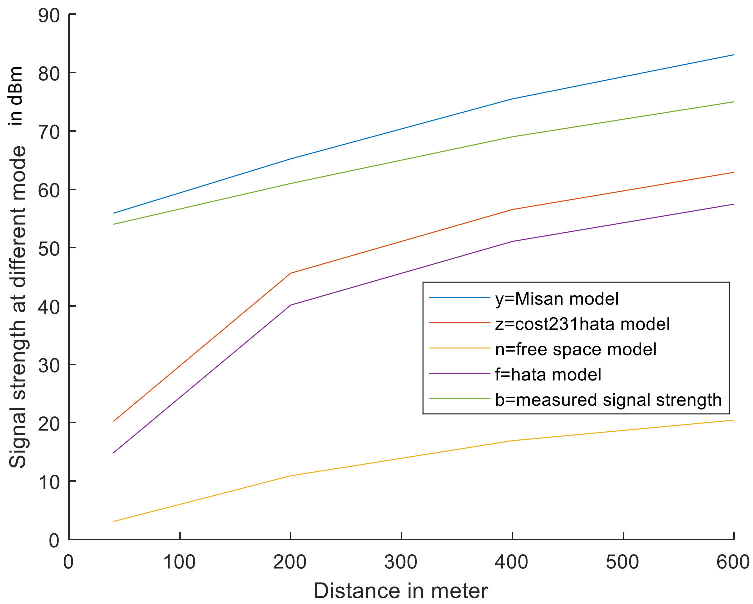

Figure 4-5 Comparison of signal strength at different models in site4.

Figures (4-2) to (4-5) display the signal strength of collected data at 2100MHz for mobile antenna heights of 1.0 meter at distances of 40, 200, 400, and 600 meters between the transmitter and receiver. Additionally, the measured signal strength is compared with the Misan model, Hata model, COST231 model, and the free space model. The comparison shows that the signal strength for the proposed model is closer to the measured signal strength than the other models. At distances ≤200 meters, the signal strength for the proposed model is much closer to the measured signal strength because the path loss is minimal and there are fewer buildings. However, for distances >200 meters, the signal strength for the proposed model starts to deviate from the measured signal strength because the path loss increases due to the presence of more buildings.

4.4 Calculation of root mean sequare error

Calculates the RMSE, which represent the difference between the measured and estimated received signal power by using Eq. (4-2) [69] :

$$\textbf{RMSE} = \sqrt{\frac{1}{N}\sum_{i=1}^{N}(p_i - \tilde{p}_i)^2} \qquad \text{..... 4-2}$$

Where:

p_i is the i-th measured received signal power.

$\tilde{p}_i$ is the i-th estimated received signal power.

Table 4-6. Comparison of RMSEs in different propagation models at different distance between transmitter and receiver for site 1 .

Distance in meter	Root Mean Squared Errors (RMSEs) in dB			
	FRPL	Cost231-Hata	Hata	Misan model
40	52.07	34.78	40.23	2.90
200	52.1	17.38	22.9	3.16
400	58.1	18.47	23.92	2.0
600	57.5	15.09	20.55	5.06

Table 4-7. Comparison of RMSEs in different propagation models at different distance between transmitter and receiver for site 2 .

Distance in meter	Root Mean Squared Errors (RMSEs) in dB			
	FRSL	Cost231-Hata	Hata	Misan model
40	56.93	39.77	45.17	2.09
200	54.1	19.4	24.84	5.16
400	52.1	12.47	17.93	5.4
600	57.56	15.08	20.55	5.06

Table 4-8. Comparison of RMSEs in different propagation models at different distance between transmitter and receiver for site 3 .

Distance in meter	Root Mean Squared Errors (RMSEs) in dB			
	FRSL	Cost231-Hata	Hata	Misan model
40	56.93	39.78	45.17	2.1
200	59.1	24.34	29.83	9.0

400	59.08	19.47	24.93	2.0
600	57.56	15.09	20.55	5.06

Table 4-9. Comparison of RMSEs in different propagation models at different distance between transmitter and receiver for site 4 .

Distance in meter	Root Mean Squared Errors (RMSEs) in dB			
	FSPL	Cost231-Hata	Hata	Misan model
40	51.93	34.78	40.17	2.9
200	50.1	15.38	20.83	2.0
400	52.08	12.47	17.93	5.4
600	54.56	12.09	17.55	8.0

It is evident from Tables (4-6), (4-7), (4-8), and (4-9) that the proposed model produces RMSEs for signal strength within the acceptable range for accurate signal prediction. The free space model, Hata model, and the COST231 – Hata model generally predict the path loss in the tested area, but their RMSEs for signal strength are significantly higher than the value for proposed model.

4.5 Signal Path Loss Calculation for 4G at 2600MHz:

Calculating signal path loss with equations (1-2), (1-9), (1-15), and (3-1). Table (4-10) shows the path loss at FSPL, COST231-Hata, Hata, and Misan models.

Table 4-10. Signal path loss in different propagation models.

Distance in meter	Path loss in dB			
	FSPL	Cost231-Hata	Hata	Misan model
40	72.7807	97.4400	91.2581	115.7154
200	86.7601	122.7703	116.5884	135.3584
400	92.7807	133.6795	127.4976	149.8477
600	96.3025	140.0609	133.8790	158.3233

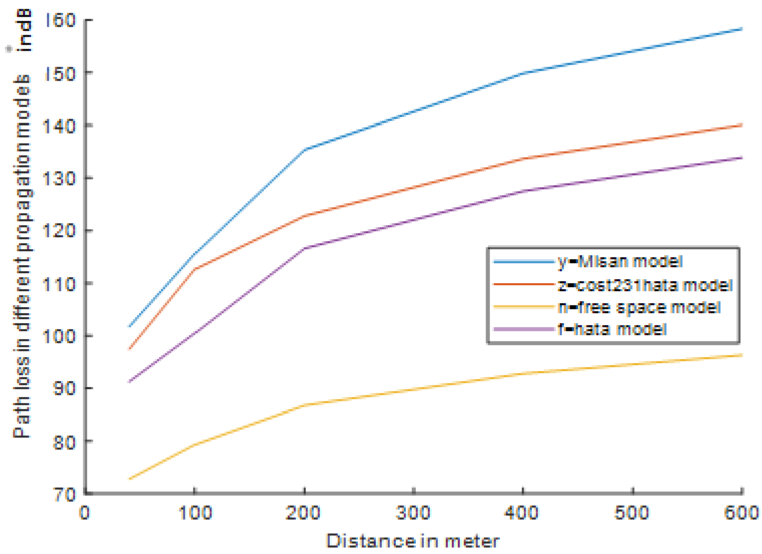

Figure 4-6 Path loss at different models.

The graph in Figure 4-6 illustrates the path loss at 2600MHz for a transmitted antenna height of 21 meter and a mobile antenna height of 1.0 meter at distances of 40, 200, 400, and 600 meter between the transmitter and receiver. In addition, the path loss for the proposed model (Misan model) is compared with the Hata model, the COST231 model, and the free space model signal strength. The comparison shows that the path loss for the proposed model is greater than for the other models. However, this results in a signal strength closer to the measured signal strength than the other models.

4.6 Signal Strength Calculation for 4G at 2600MHz

The signal strength represents the power output of a transmitter as measured by a reference antenna located far away from the transmitting antenna. The received signal strength for Misan model, Hata model , FSPL model and COST-231 model can be calculated as in Eq.(4-1)[69].

The signal strength for proposed model is closer to the measured signal strength as in Tables 4-11:

Table 4-11. Comparison of signal strength in different propagation models at different distance between transmitter and receiver for site 1 .

Distance in meter	Signal Strength in dBm				
	FSPL	Cost231-Hata	Hata	Misan model	Measured signal strength
40	-1.2193	-23.4400	-17.2581	-42.8577	-58
200	-12.7601	-48.7703	-42.5884	-61.3384	-66
400	-18.7807	-59.6795	-53.4976	-75.8477	-75
600	-22.3025	-66.0609	-59.8790	-84.3233	-79

Table 4-12. Comparison of signal strength in different propagation models at different distance between transmitter and receiver for site 2 .

Distance in meter	Signal Strength in dBm				
	FSPL	Cost231-Hata	Hata	Misan model	Measured signal strength
40	-1.2193	-23.4400	-17.2581	-42.8577	-50
200	-12.7601	-48.7703	-42.5884	-61.3384	-60
400	-18.7807	-59.6795	-53.4976	-75.8477	-69
600	-22.3025	-66.0609	-59.8790	-84.3233	-75

Table 4-13. Comparison of signal strength in different propagation models at different distance between transmitter and receiver for site 3 .

Distance in meter	Signal Strength in dBm				
	FSPL	Cost231-Hata	Hata	Misan model	Measured signal strength
40	-1.2193	-23.4400	-17.2581	-42.8577	-60
200	-12.7601	-48.7703	-42.5884	-61.3384	-70
400	-18.7807	-59.6795	-53.4976	-75.8477	-76
600	-22.3025	-66.0609	-59.8790	-84.3233	-78

Table 4-14. Comparison of signal strength in different propagation models at different distance between transmitter and receiver for site 4 .

Distance in meter	Signal Strength in dBm				
	FSPL	Cost231-Hata	Hata	Misan model	Measured signal strength
40	-1.2193	-23.4400	-17.2581	-42.8577	-65
200	-12.7601	-48.7703	-42.5884	-61.3384	-70
400	-18.7807	-59.6795	-53.4976	-75.8477	-74
600	-22.3025	-66.0609	-59.8790	-84.3233	-80

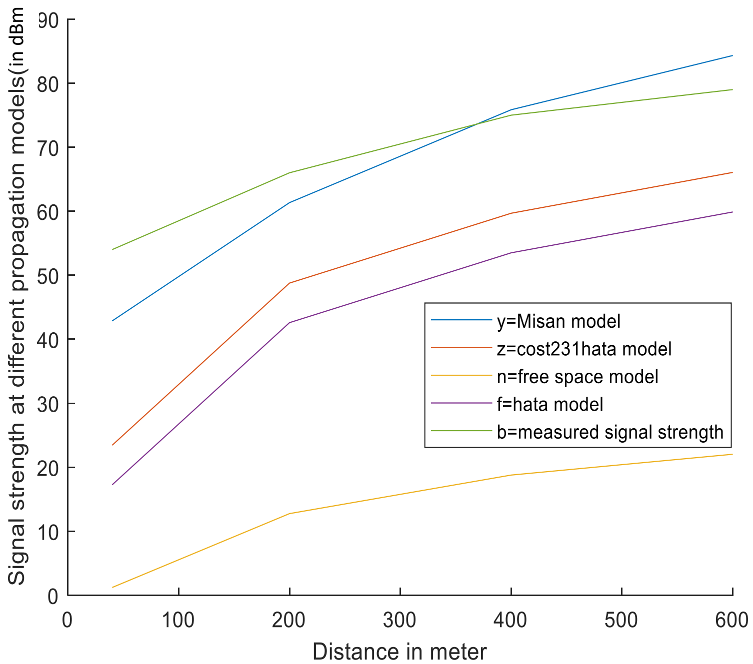

Figure 4-7 Comparison of signal strength at different models in site1.

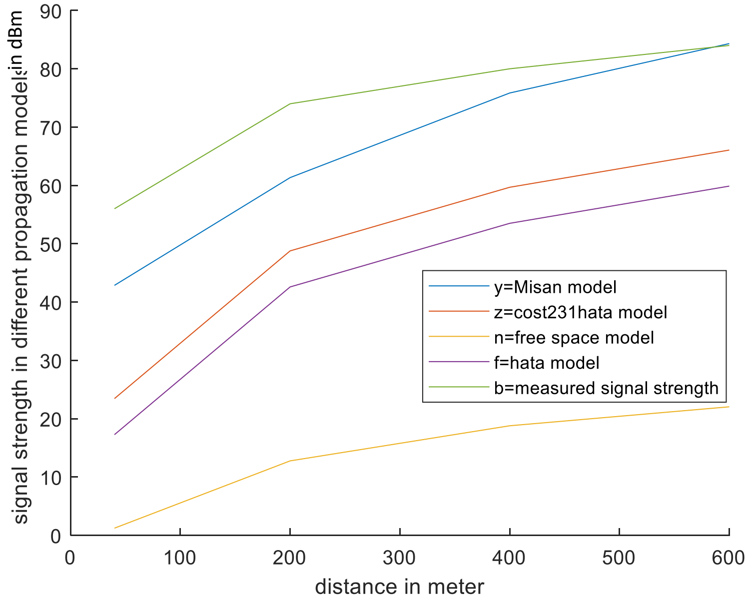

Figure 4-8 Comparison of signal strength at different models in site2.

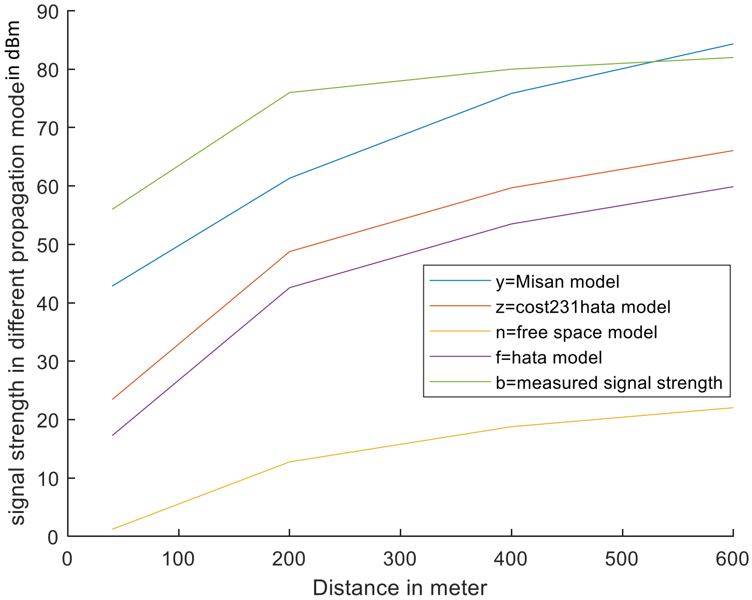

Figure 4-9 Comparison of signal strength at different models in site3.

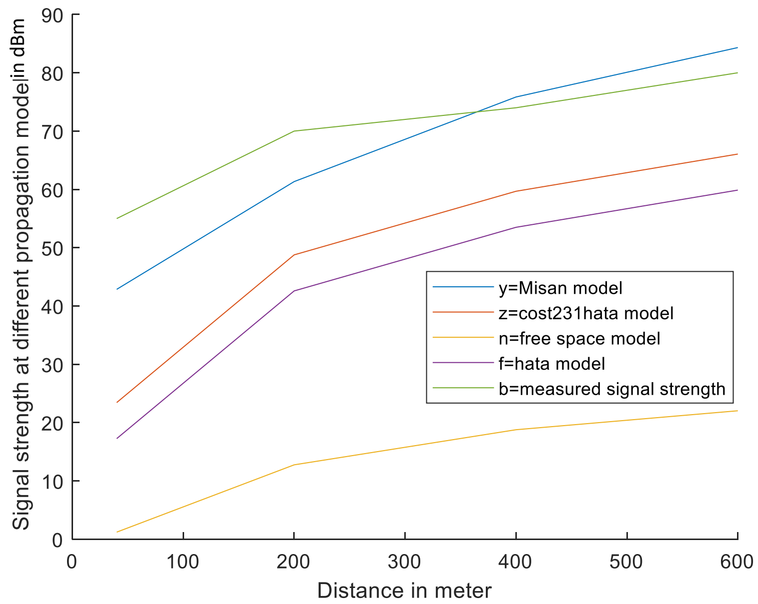

Figure 4-10 Comparison of signal strength at different models in site4.

The Figures (4-7) to (4-10) displays the signal strength of collected data at 2100MHz for mobile antenna heights of 1.0 meter at distances of 40, 200, 400, and 600 meter between the transmitter and receiver. The measured signal strength is compared with the Misan model, Hata model, COST231 model, and the free space model. The comparison shows that the signal strength for the proposed model is closer to the measured signal strength than the other propagation models. At distances ≥200 meters, the signal strength for the proposed model is much closer to the measured signal strength because the path loss is starting to increase due to the presence of many buildings. However, for distances <200 meters, the signal strength for the proposed model begins to deviate from the measured signal strength because the path has fewer buildings.

Table 4-15. Comparison of RMSEs in different propagation models at different distance between transmitter and receiver for site 1 .

Distance in meter	Root Mean Squared Errors (RMSEs) in dB			
	Free space	Cost231-Hata	Hata	Misan model
40	56.78	34.56	40.74	10.64
200	53.23	17.229	23.41	4.66
400	56.21	15.32	21.50	2.23
600	56.96	12.93	19.12	5.32

Table 4-16. Comparison of RMSEs in different propagation models at different distance between transmitter and receiver for site 2 .

Distance in meter	Root Mean Squared Errors (RMSEs) in dB			
	FSPL	Cost231-Hata	Hata	Misan model
40	54.79	32.56	38.75	9.85
200	61.24	25.23	31.42	10.12
400	61.22	20.33	26.51	4.16
600	61.97	17.94	24.13	2.32

Table 4-17. Comparison of RMSEs in different propagation models at different distance between transmitter and receiver for site 3 .

Distance in meter	Root Mean Squared Errors (RMSEs) in dB			
	FSPL	Cost231-Hata	Hata	Misan model
40	54.79	32.56	38.75	9.51
200	63.24	27.23	33.42	8.92
400	61.22	20.33	26.51	4.16
600	59.97	15.94	22.13	2.32

Table 4-18. Comparison of RMSEs in different propagation models at different distance between transmitter and receiver for site 4 .

Distance in meter	Root Mean Squared Errors (RMSEs) in dB			
	FSPL	Cost231-Hata	Hata	Misan model
40	58.93	30.78	47.75	9.91

200	57.24	21.23	27.42	8.67
400	54.22	13.33	19.51	2.84
600	57.97	13.94	20.13	4.32

It is evident from Tables 4-15 to 4-18 that the proposed model produces RMSEs for signal strength within the acceptable range for accurate signal prediction. In contrast, the Free Space model, Hata model, and the COST231 – Hata model generally overestimate the path loss in the tested area, with RMSEs for signal strength significantly exceeding the acceptable value.

Chapter Five: CONCLUSIONS AND RECOMINDATIONS

5.1 Conclusions:

Various propagation models have been thoroughly researched, analyzed, and compared. The results offer guidance in selecting a model that provides optimal and balanced outcomes. For the urban propagation environment, a proposed model has been designed and simulated compared with actual measurements.

The following are the main findings of this study:

- When comparing the predicted and measured signal levels, the RMSE for proposed model is less than other propagation models.
- The predicted signal strength is much closer to the measured signal strength.
- The proposed method can be used to predict the path loss for urban propagation environment.

5.2 Recommendations:

- Testing the proposed model for mobile communications in suburban and rural area .
- The appropriate band of the suggested model may be expanded. To do this, choose a base station that is active in a different band and perform Drive Test (DT). It is practical to model the propagation of signals at that band by altering the wavelength input during the simulation steps. If necessary, a correction factor for the new band can be determined using the RMSE comparison.
- Expanding the model to include the 5G mobile communications scenario for signal propagation prediction.

REFERENCSES

[1] M. S. Busch, *The Impact of Social Networks on Everday Life from a Psychological and a Sociological Approach*. Grin Verlag, 2016.

[2] D. Freitas, *The happiness effect: How social media is driving a generation to appear perfect at any cost*. Oxford University Press, 2017.

[3] T. Pfeifer and P. Bellavista, *Wired-Wireless Multimedia Networks and Services Management*. Springer, 2009.

[4] AIRCOM, *Radio Network Planning Fundamentals*. AIRCOM International, 2001.

[5] T. Rappaport, *Wireless Communications: Princibles and Practice*. Printice Hall, 2001.

[6] I. S. Misra, *Wireless Communications and Networks*. McGraw-Hill, 2009.

[7] R. Vaughan and J. B. Andersen, *Channels, Propagation and Antennas for Mobile Communications*. IET Electromagnetic Waves Series 50, 2003.

[8] T. K. Sarkar, Z. Ji, K. Kim, A. Medouri, and M. Salazar-Palma, "A survey of various propagation models for mobile communication," *IEEE Antennas Propag. Mag.*, vol. 45, no. 3, pp. 51–82, 2003.

[9] C. H. Papas, *Theory of electromagnetic wave propagation*. Courier Corporation, 2014.

[10] V. Garg, *Wireless communications & networking*. Elsevier, 2010.

[11] T. K. Sarkar, "The Development of Wireless Telegraphy and Telephony, and Pioneering Attempts to Achieve Transatlantic Wireless Communications," *Hist. Wireless, Wiley-IEEE Press Eb. Chapters, 2006, pp. 349 - 420.*.

[12] C. Haslett, *Essentials of radio wave propagation*. Cambridge University Press, 2008.

[13] J. Seybold, *Introduction to RF Propagation*. Wiley, 2005.

[14] C. Akkaşlı, *Methods for Path loss Prediction*. Växjö University, 2009.

[15] A. S. Abdulrasool, "Modeling and Simulation of Radio Wave Propagation Coverage for Rural Wireless Communication Systems," 2017.

[16] H. R. Anderson, *Fixed Broadband Wireless System Design*. Wiley, 2003.

[17] C. A. Balanis, *Antenna Theory Analysis and Design*. Wiley, 1989.

[18] P. O. Luthi, B. Chopard, and J.-F. Wagen, "Wave propagation in urban microcells: a massively parallel approach using the TLM method," in *International Workshop on Applied Parallel Computing*, Springer, 1995, pp. 408–418.

[19] P. Kreuzgruber, T. Brundl, W. Kuran, and R. Gahleitner, "Prediction of indoor radio propagation with the ray splitting model including edge diffraction and rough surfaces," in *Proceedings of IEEE Vehicular Technology Conference (VTC)*, IEEE, 1994, pp. 878–882.

[20] P. Beckmann and A. Spizzichino, "The scattering of electromagnetic waves from rough surfaces," *Norwood*, 1987.

[21] J. G. Proakis, *Digital Communications*. McGraw-Hill, 2001.

[22] R. Heydari, I. M. Sharifi, M. Sedghi, S. Alirezaee, and M. Ahmadi, "Effects of terrain factors in 900 MHz GSM urban cells and a pathloss estimation approach," in *2014 22nd Iranian Conference on Electrical Engineering (ICEE)*, IEEE, 2014, pp. 1555–1560.

[23] K. Rizk, J. F. Wagen, and F. Gardiol, "Two-Dimensional Ray Tracing Modeling for Propagation Prediction in Microcellular Environments," *IEEE Trans. Veh. Technol. vol. 46, no. 2, pp. 508-518*, 1997.

[24] M. Hata, "Empirical Formula for Propagation Loss in Land Mobile Radio Services," *IEEE Trans. Veh. Technol. Vols. VT-29, no. 3, pp. 317-325*, 1980.

[25] C. A. 231, "Digital Mobile Radio Towards Future Generation Systems," *Eur.*

Comm., 1999.

[26] F. Ikegami, S. Yoshida, T. Takeuchi, and M. Umehira, "Propagation Factors Controlling Mean Field Strength on Urban Streets," *IEEE Trans. Antennas Propagation, vol. 32, no. 8, p. 822–829,* 1984.

[27] H.R. Anderson, "A Ray-Tracing Propagation Model for Digital Broadcast Systems in Urban Areas," *IEEE Trans. Broadcast. vol. 39, no. 3, p. 309–317,* 1993.

[28] J. W. S. R. J. Luebbers, "Comparison of GTD and FDTD Predictions for UHF Radio Wave Propagation in a Simple Outdoor Urban Environment," *IEEE Int. Symp. Antennas Propagation, vol. 3, pp. 2022-2025*, 1997.

[29] E. Harinda, S. Hosseinzadeh, H. Larijani, and R. M. Gibson, "Comparative Performance Analysis of Empirical Propagation Models for LoRaWAN 868MHz in an Urban Scenario," *2019 IEEE 5th World Forum Internet Things*, 2019.

[30] S. I. Popoola, S. Misra, and A. A. Atayero, "Outdoor Path Loss Predictions Based on Extreme Learning Machine," *Wirel. Pers. Commun.*, vol. 99, no. 1, pp. 441–460, 2018, doi: 10.1007/s11277-017-5119-x.

[31] A. S. Khatouni, F. Soro, and D. Giordano, "A machine learning application for latency prediction in operational 4g networks," in *2019 IFIP/IEEE Symposium on Integrated Network and Service Management (IM)*, IEEE, 2019, pp. 71–74.

[32] Y. Zhang, J. Wen, G. Yang, Z. He, and J. Wang, "Path loss prediction based on machine learning: Principle, method, and data expansion," *Appl. Sci.*, vol. 9, no. 9, p. 1908, 2019.

[33] T. Nishio, H. Okamoto,K. Nakashima , and Y. Koda , "Proactive received power prediction using machine learning and depth images for mmWave networks," *IEEE J. Sel. Areas Commun.*, vol. 37, no. 11, pp. 2413–2427,

2019.

[34] S. I. Popoola, A. Jefia, A. Atayero, and O. Kingsley, “Determination of neural network parameters for path loss prediction in very high frequency wireless channel,” *IEEE access*, vol. 7, pp. 150462–150483, 2019.

[35] K. Inoue, K. Ichige, T. Nagao, and T. Hayashi, “Radio propagation prediction using deep neural network and building occupancy estimation,” *IEICE Commun. Express*, vol. 9, no. 10, pp. 506–511, 2020.

[36] H.-S. Jo, C. Park, E. Lee, H. K. Choi, and J. Park, “Path loss prediction based on machine learning techniques: Principal component analysis, artificial neural network, and Gaussian process,” *Sensors*, vol. 20, no. 7, p. 1927, 2020.

[37] T. N. T. Hayashi, “Study on radio propagation prediction by machine learning using urban structure maps,” *IEEE Antennas Propag. Mag.*, 2020.

[38] U. Masood, H. Farooq, and A. IMran, “A Machine Learning based 3D Propagation Model for Intelligent Future Cellular Networks,” *IEEE Glob. Commun. Conf.*, 2019.

[39] S. H. Alsamhi, F. Almalki, O. Ma, M. S. Ansari, and B. Lee, “Predictive estimation of optimal signal strength from drones over IoT frameworks in smart cities,” *IEEE Trans. Mob. Comput.*, 2021.

[40] K. C. Igwe, O. D. Oyedum, A. M. Aibinu, M. O. Ajewole, and A. S. Moses, “Application of artificial neural network modeling techniques to signal strength computation,” *Heliyon*, vol. 7, no. 3, 2021.

[41] F. Jamil, N. Iqbal, S. Ahmad, and D.-H. Kim, “Toward accurate position estimation using learning to prediction algorithm in indoor navigation,” *Sensors*, vol. 20, no. 16, p. 4410, 2020.

[42] T. Nakanishi, K. Shimizu, K. Hitomi, Y. Nishioka, and Y. Inasawa, “Prediction of indoor radio propagation using deep neural network,” *IEICE*,

2023.

[43] S. H. Alsamhi, O. Ma, and M. S. Ansari, “Predictive estimation of the optimal signal strength from unmanned aerial vehicle over internet of things using ANN,” *arXiv Prepr. arXiv1805.07614*, 2018.

[44] A. Kulkarni, A. Seetharam, A. Ramesh, and J. D. Herath, “Deepchannel: Wireless channel quality prediction using deep learning,” *IEEE Trans. Veh. Technol.*, vol. 69, no. 1, pp. 443–456, 2019.

[45] M. Ozturk, M. Gogate, O. Onireti, A. Adeel, A. Hussain, and M. A. Imran, “A novel deep learning driven, low-cost mobility prediction approach for 5G cellular networks: The case of the Control/Data Separation Architecture (CDSA),” *Neurocomputing*, vol. 358, pp. 479–489, 2019.

[46] M. Alrabeiah and A. Alkhateeb, “Deep learning for mmWave beam and blockage prediction using sub-6 GHz channels,” *IEEE Trans. Commun.*, vol. 68, no. 9, pp. 5504–5518, 2020.

[47] T. Hayashi, T. Nagao, and S. Ito, “A study on the variety and size of input data for radio propagation prediction using a deep neural network,” in *2020 14th European Conference on Antennas and Propagation (EuCAP)*, IEEE, 2020, pp. 1–5.

[48] X. Zhang, X. Shu, B. Zhang, J. Ren, L. Zhou, and X. Chen, “Cellular network radio propagation modeling with deep convolutional neural networks,” in *Proceedings of the 26th ACM SIGKDD International Conference on knowledge discovery & data mining*, 2020, pp. 2378–2386.

[49] J. Thrane, B. Sliwa, C. Wietfeld, and H. L. Christiansen, “Deep Learning-based Signal Strength Prediction Using Geographical Images and Expert Knowledge,” *GLOBECOM 2020 - 2020 IEEE Glob. Commun. Conf.*, 2020.

[50] J. Thrane, D. Zibar, and H. L. Christiansen, “Model-Aided Deep Learning Method for Path Loss Prediction in Mobile Communication Systems at 2.6

GHz," *IEEE Access*, vol. 8, 2020.

[51] L. Wu, D. He, B. Ai, J. Wang, "Artificial neural network based path loss prediction for wireless communication network," *IEEE access*, vol. 8, pp. 199523–199538, 2020.

[52] B. Kim, Y. Sagduyu, T. Erpek, and S. Ulukus, "Adversarial attacks on deep learning based mmWave beam prediction in 5G and beyond," in *2021 IEEE Statistical Signal Processing Workshop (SSP)*, IEEE, 2021, pp. 590–594.

[53] E. Krijestorac, S. Hanna, and D. Cabric, "Spatial Signal Strength Prediction using 3D Maps and Deep Learning," *IEEE Int. Conf. Commun.*, 2021.

[54] S. Mohammadjafari, S. Roginsky, E. Kavurmacioglu, M. Cevik, J. Ethier, and A. B. Bener, "Machine learning-based radio coverage prediction in urban environments," *IEEE Trans. Netw. Serv. Manag.*, vol. 17, no. 4, pp. 2117–2130, 2020.

[55] R. Levie, Ç. Yapar, G. Kutyniok, and G. Caire, "RadioUNet: Fast radio map estimation with convolutional neural networks," *IEEE Trans. Wirel. Commun.*, vol. 20, no. 6, pp. 4001–4015, 2021.

[56] O. Ozyegen, S. Mohammadjafari, M. Cevik, K. El Mokhtari, J. Ethier, and A. Basar, "An empirical study on using CNNs for fast radio signal prediction," *SN Comput. Sci.*, vol. 3, no. 2, p. 131, 2022.

[57] J. Isabona, A. Imoize, S. Ojo , and O. Karunwi , "Development of a multilayer perceptron neural network for optimal predictive modeling in urban microcellular radio environments," *Appl. Sci.*, vol. 12, no. 11, p. 5713, 2022.

[58] B. Yamamoto, A. Wong, P. Agcanas, and K. Jones , "Received signal strength indication (RSSI) of 2.4 GHz and 5 GHz wireless local area network systems projected over land and sea for near-shore maritime robot operations," *J. Mar. Sci. Eng.*, vol. 7, no. 9, p. 290, 2019.

[59] F. Hossain, T. K. Geok, T. A. Rahman, M. N. Hindia, K. Dimyati, and A. Abdaziz, "Indoor millimeter-wave propagation prediction by measurement and ray tracing simulation at 38 GHz," *Symmetry (Basel).*, vol. 10, no. 10, p. 464, 2018.

[60] F. Hossain, T. Geok , T. Rahman , M. Hindia , and K. Dimyati, "An efficient 3-D ray tracing method: Prediction of indoor radio propagation at 28 GHz in 5G network," *Electronics*, vol. 8, no. 3, p. 286, 2019.

[61] Mingjie Pang; Han Wang; Kaiwei Lin; Hai Lin, "A GPU-Based Radio Wave Propagation Prediction With Progressive Processing on Point Cloud," *IEEE Antennas Propag. Mag.*, 2021.

[62] J. Isabona, "Wavelet generalized regression neural network approach for robust field strength prediction," *Wirel. Pers. Commun.*, vol. 114, no. 4, pp. 3635–3653, 2020.

[63] E. Alimpertis, A. Markopoulou, C. Butts, and K. Psounis, "City-wide signal strength maps: Prediction with random forests," in *The World Wide Web Conference*, 2019, pp. 2536–2542.

[64] Z. K. Adeyemo, T. O. Olawuyi, O. F. Oseni, and S. I. Ojo, "Development of a Path-loss Prediction Model Using Adaptive Neuro-fuzzy Inference System," *Int. J. Wirel. Microw. Technol.*, vol. 9, no. 6, pp. 40–53, 2019.

[65] L. Huang, X. Wu, Z. Li, Y. Lu, M. Wang, and Y. Long, "A parallel FDTD/ADI-PE method for ultralarge-scale propagation modeling of ILS signal analysis," *IEEE Antennas Wirel. Propag. Lett.*, vol. 19, no. 12, pp. 2245–2249, 2020.

[66] A. A. H. Budalal, M. R. Islam, K. Abdullah, and T. A. Rahman, "Modification of distance factor in rain attenuation prediction for short-range millimeter-wave links," *IEEE Antennas Wirel. Propag. Lett.*, vol. 19, no. 6, pp. 1027–1031, 2020.

[67] H. Singh, V. Kumar, K. Saxena, and B. Bonev, "An Intelligent model for prediction of attenuation caused by rain based on machine learning techniques," in *2020 international conference on contemporary computing and applications (IC3A)*, IEEE, 2020, pp. 92–97.

[68] A. E. Ibhaze, S. O. Ajose, A. A.-A. Atayero, and F. E. Idachaba, "Developing smart cities through optimal wireless mobile network," in *2016 IEEE International Conference on Emerging Technologies and Innovative Business Practices for the Transformation of Societies (EmergiTech)*, IEEE, 2016, pp. 118–123.

[69] C. Temaneh-Nyah and J. Nepembe, "Determination of a suitable correction factor to a radio propagation model for cellular wireless network analysis," in *2014 5th International Conference on Intelligent Systems, Modelling and Simulation*, IEEE, 2014, pp. 175–182.

Appendix A

- Matlab program of Free Space Path Loss

```
function loss=freespace(frequency, distance)
%
% Inputs:

%   frequency : Carrier frequency (in MHz)
%   distance :  distance between tx and rx (in km,
should be >1)
%
% Ouputs :
%   loss : Signal loss (in dB)

% warn if the any distances are below 1 km (the model
will still give an
% output, you will have been warned that it may be in
error)
if length(find(distance<1))~=0
    fprintf('WARNING - distance set below 1km in
freespace loss\n');
end

loss=32.44 + -10logGT-10logGR +20*log10(frequency) +
20*log10(distance);
```

- Path Loss Matlab Program of Hata Model

```
function loss=hata(frequency, txhgt, rxhgt, range,
landtype)

% this function calculates the loss due to an urban,
suburban or open area
% using Hata's approximation to Okumura's method.
%
% Note : Any one input can be a vector (except
landtype).

%   Corrected an error with rxhgt a vector and large
city
%
% Inputs :
%   frequency   carrier frequency (MHz)
%   txhgt       height of transmitter (m)
%   rxhgt       height of receiver (m)
%   range       distance between transmitter and
receiver (km)
%   landtype    1=large city
%               2=small or medium city
%               3=suburban
%               4=open ground
%
% Example call (will plot out loss from 1-20km for
900MHz signal)
%   plot([1:20], hata(900, 150, 1.5, [1:20], 1))

% check values of inputs and issue warnings
if length(find(frequency<150 | frequency>3000))~=0
    fprintf('WARNING - frequency out of 150-3000 MHz
range\n');
end

if length(find(txhgt<20 | txhgt>200))~=0
    fprintf('WARNING - tx height out of 20-200m
range\n');
```

```
end

if length(find(rxhgt<1 | rxhgt>10))~=0
    fprintf('WARNING - rx height out of 1-10m
range\n');
end

if landtype<1 | landtype>4
    fprintf('ERROR - landtype should be in range 1 to
4\n');
    return
end

% correction factor for mobile antenna height
if landtype==1
    if length(find(frequency>200 & frequency<400))~=0
        fprintf(['ERROR - Cannot use frequency in
range', ...
            ' 200-400MHz with large city\n']);
        return
    end
    if length(rxhgt)~=1 % assumes that frequency is a
scalar
        if frequency<=200
            ahr=8.29*(log10(1.54*rxhgt)).^2-1.1;
        elseif frequency>=400
            ahr=3.2*(log10(11.75*rxhgt)).^2-4.97;
        end
    else    % if frequency is a vector, then rxhgt
should be a scalar
        temp=find(frequency<=200);
        if length(temp)~=0
            ahr(temp)=8.29*(log10(1.54*rxhgt)).^2-1.1;
        end
        temp=find(frequency>=400);
        if length(temp)~=0
            ahr(temp)=3.2*(log10(11.75*rxhgt)).^2-4.97;
        end
    end
else
```

```
    ahr=(1.1*log10(frequency)-0.7)*rxhgt-
(1.56*log10(frequency)-0.8);
end

urbanloss=69.55+26.16*log10(frequency)-
13.82*log10(txhgt)-ahr+...
    (44.9-6.55*log10(txhgt))*log10(range);

if landtype==1 | landtype==2
    loss=urbanloss;
elseif landtype==3
    loss=urbanloss-2*log10(frequency/28).^2-5.4;
elseif landtype==4
    loss=urbanloss-
4.78*log10(frequency).^2+18.33*log10(frequency)-40.94;
end
```

- Matlab Program of Cost231-Hata

```
function loss=cost231hata(frequency, txhgt, rxhgt,
range, citysize)

% this function calculates the loss due to an urban
area using the COST231
% extension to the hata model for frequencies 1500-
2500MHz.
%
% Note : Any one input can be a vector (except
citysize)

% Inputs :
%   frequency    carrier frequency (MHz)
%   txhgt        height of transmitter (m)
%   rxhgt        height of receiver (m)
%   range        distance between transmitter and
receiver (km)
%   citysize     large (=1) or medium or small (=2)
%
```

```
% check values of inputs and issue warnings
if length(find(frequency<1500 | frequency>3000))~=0
    fprintf('ERROR - frequency out of 1500-3000 MHz
range - use hata\n');
    return
end

if length(find(txhgt<20 | txhgt>200))~=0
    fprintf('WARNING - tx height out of 20-200m
range\n');
end

if length(find(rxhgt<1 | rxhgt>10))~=0
    fprintf('WARNING - rx height out of 1-10m
range\n');
end

if citysize<1 | citysize >2
    fprintf('ERROR - unknown city size\n');
    return
end

% correction factor for mobile antenna height
if citysize==1
    temp=find(frequency>=400);
    if length(temp)~=0
        ahr(temp)=3.2*(log10(11.75*rxhgt)).^2-4.97;
    end
    C=3;
else
    ahr=(1.1*log10(frequency)-0.7)*rxhgt-
(1.56*log10(frequency)-0.8);
    C=0;
end
loss=46.3+33.9*log10(frequency)-13.82*log10(txhgt)-
ahr+...
    (44.9-6.55*log10(txhgt))*log10(range)+C;
```

- Path Loss Matlab Program of Proposed Model

```
function loss=Misan(frequency, ht, hr, d, n0, n1, n2,
n3)
% this function calculates the loss due to an urban
area using the ericsson

% Note : Any one input can be a vector


% Inputs :
%   frequency   carrier frequency (MHz)
%   ht       height of transmitter (m)
%   hr       height of receiver (m)
%   d        distance between transmitter and receiver
(km)
%
loss=a0+a1*log10(d)+a2*log10(ht)+a3*log10(ht)-
3.2*(log10(11.75*hr))^2+45.1*log10(frequency);

end
```

Appendix B

List of Publications

[1] N.A.Abdullrazaq, H.A.AL-Behadili, "A Comprehensive Review of Radio Signal Propagation Prediction for Terrestrial Wireless Communication Systems," Misan Journal of Engineering Sciences, Vol. 3, No. 1, June 2024, ISSN: 2957-4250.

[2] N.A.Abdullrazaq, H.A.AL-Behadili, "Predicting The Path Loss at the Receiver for 4G Communications 2600MHz Using Mathematical Model in Amara City," Accepted for publication in IEEE conference International Symposium of Systems, Advanced Technologies and Knowledge ISSATK, 2-3 Nov 2024 Kairouan (Tunisia). **(Scopus)**

[3] N.A.Abdullrazaq, H.A.AL-Behadili, "Statistical Propagation Model for Path Loss Prediction in Amara City for 3G Communications at 2100MHz," Under reviewing in 3rd International Conference on Engineering and Science to Achieve the Sustainable Development Goals, 25 - 26 September 2024 | Istanbul, Turkey.**(Scopus)**

Misan Journal of Engineering Sciences
Vol. 3, No. 1, July 2024

ISSN: 2957-4250
ISSN-E: 2957-4242

A Comprehensive Review of Radio Signal Propagation Prediction for Terrestrial Wireless Communication Systems

Nabaa A. Abdullrazaq[1*] and Hasanain A. H. Al-Behadili[1]
[1] *Department of Electrical Engineering, College of Engineering, University of Misan, Maysan, Iraq.*
Corresponding author E-mail: enghre.2201@uomisan.edu.iq

(Received 4 May, Revised 20 May, Accepted 21 May)

Abstract: The subject of study known as radio propagation prediction refers to predicting the behaviour and characteristics of radio waves as they propagate through the atmosphere. It is a basic element of all wireless communication systems, including satellite communications, broadcasting and cellular networks. While there is no study covers all the techniques used to predict the radio signal prediction, this study presents a review of the propagation prediction models between 2018-2023 used for terrestrial wireless communication systems; the classic empirical models were briefly explained, followed by the deterministic propagation models that have been developed using ray-tracing with deep and machine learning techniques. Recent studies on an improvement of the computational efficiency and accuracy of propagation prediction models were also reviewed, in addition to an overview of some of the traditional statistical models. Furthermore, some of the new techniques in propagation prediction were described. The results of these studies explain that techniques using ray tracing produce better results than other techniques.

Keywords: Machine learning techniques; Neural Network technique; propagation prediction models; Terrestrial wireless communication systems; Computational efficiency.

1. Introduction

Mobile wireless communication devices have impacted our daily lives in different ways as they have facilitated human commerce, lifestyle, and social interaction through unrestricted global communication [1],[2]. Companies/operators offer these wireless network services for both non-real-time activities like web browsing to real-time ones like phone and video calls [3]. Performance measures exist for both real-time and non-real-time services. Wireless network operators can maintain and improve network performance while staying within acceptable bounds thanks to these performance measures [4]. By attracting more users and consequently more assets, this respectable performance will keep them from breaking the license regulatory contract.

One of the performance metrics can be the ability to forecast signal propagation in the wireless network with accuracy depending on the design of the network. The primary benefit of prediction is that it is less expensive than field measurements [5]. From one environment to another, the accuracy of propagation models differs significantly and the variance from the propagation model's application context is different from the environment in which it was developed. When these models are used in some nations, the outcomes are disheartening and misleading, leading to an inadequate network design [6]. For instance, several commonly used propagation models, such as Okumura, Hata, etc. when employed in particular cases, such as Japanese cities, can provide extremely good accuracy, but when used in other environments, such as European cities, they will not perform optimally [7]. Other models from the site-specific class, such as Finite-Difference Time-Domain (FDTD), can provide extremely precise findings regardless of the propagation environment, but their applications are restricted by the enormous computation and lengthy prediction times needed for small areas [8].

DOI: https://doi.org/10.61263/mjes.v3i1.80

ISSATK2024 notification for paper 22

خارجي البريد الوارد

ISSATK2024 ٤:٠٦ م

إلى أنا

الترجمة إلى العربية

Dear Authors,

Congratulations! Your paper number 22 has been accepted

We are pleased to inform you that your paper titled Predicting The Path Loss at the Receiver for 4G Communications 2600MHz Using Mathematical Model in Amara City has been accepted for presentation at the ISSATK 2024, which will be held in Kairouan, Tunisia from 2 to 3 november 2024.

We received a large number of high-quality submissions this year, and your work was selected after a rigorous peer-review process. Congratulations on this remarkable achievement!

جمهورية العراق
وزارة التعليم العالي والبحث العلمي
جامعة ميسان / كلية الهندسة
قسم الهندسة الكهربائية

تـقنية مـحسـنة لـدعم الـتـنـبؤ بـإشارة الأتـصـالات

من قبل

نبأ علي عبدالرزاق

بكالوريوس هندسة كهرباء 2011

رسالة

مقدمة الى كلية الهندسة في جامعة ميسان

كجزء من متطلبات الحصول على درجة الماجستير في علوم الهندسة الكهربائية

محرم 1446 هـ

بأشراف

الأستاذ المساعد الدكتور : حسنين عباس حسن

الــخـلاصــة

التنبؤ بالانتشار الراديوي هو عملية تنبؤ بالكيفية التي تتصرف بها الإشارات الراديوية وهي تنتقل عبر الفراغ أو الغلاف الجوي من نقطة إلى أخرى. ونماذج الانتشار الدقيقة ضرورية لتصميم الشبكات اللاسلكية وتحقيق الاستخدام الأمثل لها. غير أن العديد من النماذج النظرية والتجريبية والخاصة بمواقع محددة لها قيود تحد من فائدتها في هذا الصدد.

ولحساب قوة الإشارة في جهاز الاستقبال، من الضروري التنبؤ بفقد المسار باستخدام نماذج تنبؤ الأنتشار الراديوي. وأقترحت هذه الدراسة نموذجاً للأنتشار يوفر دقة جيدة في الاتصالات 3G و 4G في بيئة العراق / محافظة ميسان / مدينة العمارة. وشملت الدراسة أربع مواقع في مناطق مختلفة داخل مدينة العمارة. هذه المناطق تتميز بمناخها الجاف وتحتوي على بنايات تتفاوت في الأرتفاع, هذه البنايات بمعدل طابقين الى ثلاث طوابق .

تم جمع البيانات باستخدام الفحص الميداني. وقدم النموذج المقترح نتائج أفضل من نماذج الانتشار التجريبية الأخرى المستخدمة في هذه الدراسة. ويبيّن النموذج أن متوسط الجذر التربيعي للخطأ (RMSE) أقل من النماذج الأخرى (هاتا وكوست 231) عند ارتفاع الهوائي المستلم البالغ 1.0م على مسافات تبلغ 40 و200 و400 و600 متر بين جهاز الإرسال وجهاز الاستقبال فقد كانت قيمة متوسط الجذر التربيعي للخطأ عند مسافة 600 متر تتراوح بين 2.3 و 5.3. وستساعد هذه النتائج على تحسين أداء النظام إلى أقصى حد عن طريق تجديد تخطيط الترددات اللاسلكية وتصميم النظم، والتقليل إلى أدنى حد من أوجه القصور الكامنة في الشبكة مثل المكالمات الفائتة، والمسائل المتعلقة بالجودة، والتسليم، والمسائل ذات الصلة.

ويمكن استخدام النموذج المقترح للتنبؤ بخسائر المسار وتوصيف القنوات، بما في ذلك استخدام بارامترات قنوات مماثلة لتحليل الاتصالات اللاسلكية في بيئات متنقلة مختلفة. وقد تحتاج نماذج الانتشار الأخرى، مثل هاتا وكوست 231، التي لم تعطي نتائج دقيقة للتنبؤ بفقدان المسار، إلى مزيد من التطوير في المستقبل. وأشار التحليل إلى أن متوسط الجذر التربيعي للخطأ كان ضمن الحدود المسموح بها.

واستخدمت الدراسة عدة مجموعات برامجية، بما في ذلك نظام TEMS ، وبرنامج MapInfo, وبرنامج Google Earth Pro ، وبرنامج MATLAB 2020 ، لأغراض القياسات الميدانية، وتجهيز البيانات، والمحاكاة، وتحليل النتائج.